Journal of Industrial and Management Optimization

JIMO, 22(8): 3699−3740.
DOI: 10.3934/jimo.2026133
Received: 20 March 2026
Revised: 13 June 2026
Accepted: 03 July 2026
Published: 15 July 2026

https://www.aimspress.com/journal/jimo

Research article

An integrated decision framework and optimization model to forward deployment and rearward movement in city public emergency events

Shuanglin Li* **and Peiyu Kuang**

School of Traffic & Transportation Engineering, Central South University, Changsha, Hunan 410075, P. R. China

* **Correspondence:** Email: lishuanglin@csu.edu.cn.

Abstract: Integrating forward deployment and rearward movement is a challenge in city public emergency events. An integrated decision framework and optimization model were constructed to minimize response completion time in the first stage and to improve treatment effectiveness in the second stage. A hybrid solution approach combining a genetic algorithm and dynamic programming was developed to address the coordinated rescue-dispatch problem in the first stage and the hospital medical-resource scheduling problem in the second stage. A real-world case study and sensitivity analyses were conducted to evaluate the effectiveness and applicability of the proposed framework. The results show that the proposed approach can reduce emergency-vehicle deployment requirements compared with reference dispatch configurations. Furthermore, the sensitivity analyses reveal that learning and fatigue effects have a significant impact on emergency medical scheduling. Incorporating learning effects improves system performance, whereas fatigue effects tend to reduce operational efficiency during prolonged rescue operations. When both effects are considered simultaneously, coordinated scheduling yields superior overall system performance. The proposed framework provides practical decision support for integrated urban emergency response under resource and traffic constraints.

Keywords: city public emergency event; integrated decision framework; search and rescue teams forward deployment; injured rearward movement; medical resource scheduling; framework effectiveness
Mathematics Subject Classification: 90B06, 90B80, 90C27, 90C39

1. Introduction

Rapid urbanization and high population density have made modern cities more vulnerable to a wide range of emergencies—including natural disasters, urban fires, structural collapses, traffic accidents, and crowd crush incidents during large-scale public events. Such emergencies are typically characterized by uncertainty, sudden onset, and rapid escalation, thereby requiring the swift mobilization of emergency resources at the incident site, followed by the timely evacuation and distribution of casualties across multiple healthcare facilities. The end-to-end operational chain—from forward-deployed search-and-rescue teams to rearward medical transport and triage—involves coordinated action among fire and rescue services, emergency management agencies, traffic police, and medical institutions, constituting a complex, multi-stage, multi-agency decision-making process.

Major city emergencies in recent years—including the September 11, 2001 terrorist attacks in the United States, which underscored the critical need for resilient emergency operations centers amid catastrophic infrastructure failure [1]; the Itaewon crowd crush in South Korea in 2022, which revealed substantial challenges in on-site medical response and real-time communication within densely populated urban environments [2]; residential building collapses and expressway accidents in China between 2022 and 2024; and large-scale urban fires—exhibit shared characteristics: sudden population aggregation, rapid risk escalation, and sharp surges in demand for emergency services and medical care. Existing studies have shown that effective emergency response depends heavily on coordinated decision-making across multiple interrelated domains, including rescue routing, traffic management, triage operations, hospital admission capacity, and dynamic medical-resource allocation [3,4]. Similar coordination challenges also arise during emergency preparedness and planning for large-scale urban events. In this context, scenario-based simulations are increasingly employed to inform evidence-based decisions regarding security staffing levels, deployment of mobile medical posts, and integrated traffic management strategies. Notably, recent medical and behavioral studies indicate that learning effects and fatigue among healthcare personnel significantly influence both treatment efficiency and patient safety under sustained high workloads [5,6]. These findings highlight the importance of explicitly incorporating human behavioral factors into dynamic medical-resource allocation models.

From this perspective, the effectiveness of urban emergency response systems depends not only on the availability of emergency resources but also on the extent to which these resources are coordinated across different operational stages. In practice, public emergency response unfolds as a time-sensitive, sequential process, wherein on-site rescue operations and subsequent in-hospital treatment are governed by fundamentally divergent decision priorities, operational constraints, and performance metrics [7]. This inherent functional heterogeneity implies that any integrated response strategy must explicitly differentiate the objectives, resource interdependencies, and key performance drivers at each stage, while simultaneously preserving system-wide coherence and interoperability [8−10]. Against this backdrop, interagency coordination between fire and medical services exhibits pronounced stage-dependent dynamics, underscoring the need for a structured, multi-stage decision-making framework to analyze and optimize emergency operations.

The integrated workflow and temporal progression of these two phases are clearly delineated in Figure 1. In public emergency response, coordination between fire services and medical departments varies significantly across operational stages. During the initial stage, characterized by concurrent firefighting and pre-hospital medical rescue, time is the paramount determinant of survival outcomes; thus, minimizing the response completion time, i.e., the latest arrival time of all required rescue resources, emerges as the overriding objective. To enhance coordination efficiency, strategically deploying geographically proximate fire units and hospitals proves highly effective. Such proximity enables rapid mobilization and immediate initiation of life-saving interventions at the incident scene [11,12]. Concurrently, selecting hospitals strategically located relative to the incident site can reduce ambulance travel time, thereby shortening the transfer interval between the incident scene and definitive medical care [13]. Furthermore, rational traffic control plays a crucial role during rescue operations [14]. Especially at intersections with traffic lights near the accident site, proper traffic regulation effectively prevents rescue delays and maximizes rescue efficiency.

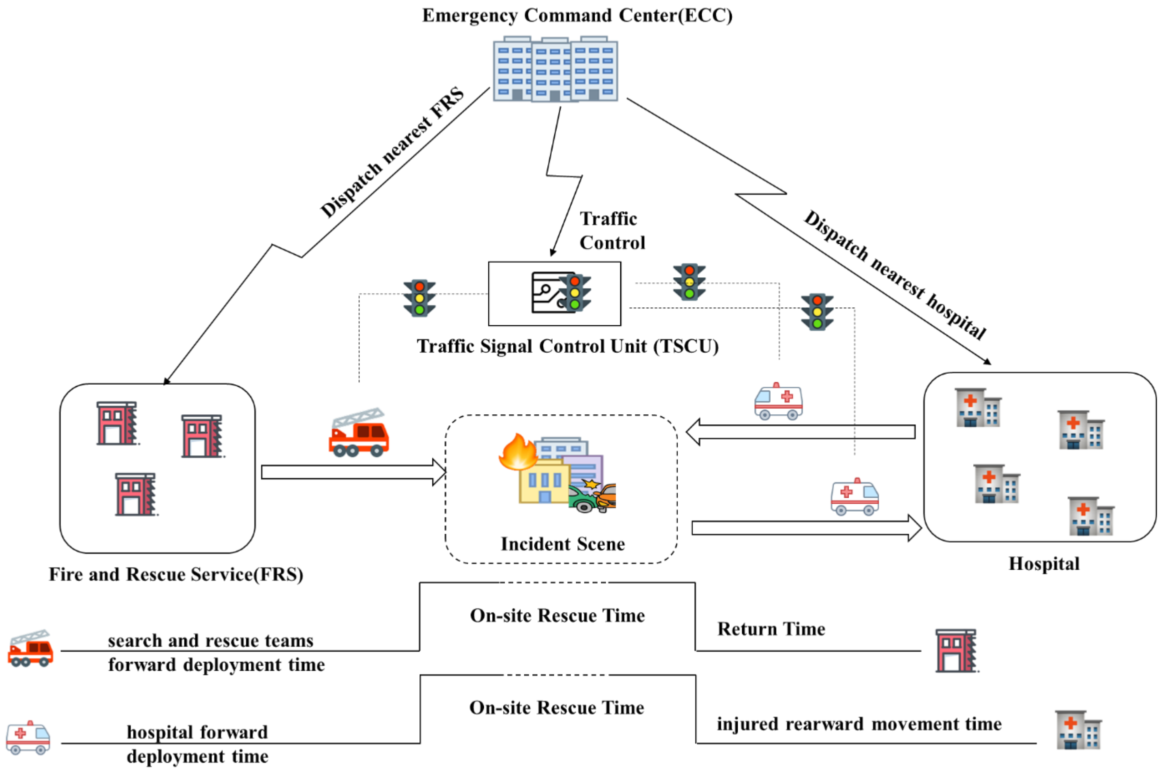

Figure 1. Two-stage rescue timeline diagram.

In the second stage, patient transfer to hospitals emphasizes the optimization of medical resource allocation and the maximization of treatment benefits. Upon arrival, patients are triaged and treated according to injury severity. Given the inherent constraints on hospital capacity, efficient utilization of available resources—ensuring timely, appropriate, and equitable care—is paramount [15,16]. Ambulance dispatch and destination assignment must therefore explicitly incorporate real-time hospital admission capacity to minimize pre-treatment waiting times. During the in-hospital treatment phase, hospitals—as specialized medical institutions—dynamically reallocate personnel, equipment, and bed capacity in response to the volume and acuity of incoming patients [17]. The scarcity of critical resources necessitates rational, adaptive scheduling by clinical teams under high-stakes, time-sensitive conditions to ensure that each patient receives the most clinically appropriate intervention [17]. Notably, physician performance is influenced by two countervailing mechanisms: prolonged and intensive clinical engagement fosters experiential learning that can improve diagnostic accuracy and procedural efficiency yet simultaneously induces physiological and cognitive fatigue that may compromise the quality of decision-making and patient safety [15,18]. Consequently, the core objective of this paper's second stage is to maximize aggregate treatment benefit through intelligent, adaptive, and equity-aware resource allocation.

The main contributions of this study are summarized as follows: (1) An integrated decision framework is proposed to coordinate fire-service dispatch, hospital dispatch, route selection, traffic control, and in-hospital medical-resource scheduling in accordance with the emergency response timeline. The framework enhances coordination between rescue agencies and healthcare institutions, thereby improving the overall efficiency of emergency operations. (2) A two-stage optimization model is developed. In the first stage, a coordinated dispatch and traffic-control model is formulated to minimize the response completion time of search-and-rescue operations. In the second stage, a dynamic medical-resource scheduling model is established to maximize the overall treatment benefit. (3) Human factors, including learning effects and fatigue effects, are explicitly incorporated into the dynamic medical-resource scheduling model. Their individual and combined impacts on treatment performance are systematically investigated. (4) A tailored genetic algorithm (GA) is developed to solve the first-stage coordinated dispatch problem involving resource allocation, route selection, and traffic control. In addition, a dynamic programming (DP) approach is proposed to address the second-stage medical-resource scheduling problem.

The remainder of this paper is organized as follows: Section 2 reviews the relevant literature. Section 3 presents the proposed coordinated rescue-dispatch model and dynamic medical-resource scheduling model. Section 4 introduces the solution methodologies, including the genetic algorithm and dynamic programming approach. Section 5 describes the case study and sensitivity analyses and discusses the computational results. Finally, Section 6 concludes the paper and outlines potential directions for future research.

2. Related literature

2.1. Emergency collaborative dispatch and traffic control in public emergency events

Effective urban emergency response depends critically on the coordination of rescue teams and logistical resources under constrained transportation conditions. Existing studies reveal a gradual transition from isolated traffic-control strategies toward integrated decision-making frameworks at the transportation-network level. Early studies predominantly sought to enhance the mobility of emergency vehicles. For instance, Su et al. (2023) adopted a multi-agent reinforcement learning framework to jointly optimize routing and signal control in an end-to-end manner [19], while Cao et al. (2022) introduced the "Gain with No Pain" concept to ensure emergency vehicle priority with minimal disruption to background traffic [20]. Building on this foundation, recent analyses highlight a shift from intersection-specific priority schemes to cooperative, network-wide traffic management supported by connected-vehicle technologies and edge-computing infrastructures (Hao et al., 2024) [21].

Meanwhile, increasing attention has been devoted to integrating traffic management with emergency logistics and evacuation planning, resulting in more comprehensive and mission-oriented decision-support frameworks. Fiedrich et al. (2000) developed one of the earliest optimization models for emergency resource allocation after earthquake disasters [22]. Auf der Heide (2006) emphasized that disaster planning and emergency resource management should be supported by evidence-based decision-making rather than solely relying on experience [23]. Subsequently, Caunhye et al. (2012)

systematically reviewed optimization models in emergency logistics and summarized major research directions in the field [24]. Rodríguez-Espíndola et al. (2023) further investigated humanitarian logistics optimization models from the perspective of decision-maker involvement and discussed future directions for improving practical implementation [25]. Wu and Gao (2021) proposed a multidimensional framework to enhance regional transport resilience [26], whereas Qin et al. (2018) developed a reliability-constrained optimization model for the strategic layout of emergency resources [27]. Focusing on distribution efficiency in emergency logistics, Liu et al. (2022) optimized urban emergency supply distribution routes to enable a rapid response to demand surges during epidemic outbreaks [28]. To jointly address prepositioning strategies and network resilience, Caunhye et al. (2016) introduced a location-routing model for emergency supply distribution; more recently [29], Valaei et al. (2026) investigated the robust prepositioning and allocation of maritime search and rescue vessels under incident location uncertainty, extending prepositioning strategies to maritime emergency operations [30]. Hu et al. (2025) designed a robust emergency logistics network capable of accommodating pandemic-induced demand uncertainty [31].

Genetic algorithms have been widely applied to solve complex optimization problems due to their strong global search capability and robustness. Yan et al. (2023) developed a hybrid metaheuristic algorithm for the multi-objective location-routing problem in the early post-disaster stage [32]. More recently, Gu et al. (2026) proposed a critical task aggregation-based NSGA-II algorithm for multi-objective early-warning mission planning, further demonstrating the effectiveness of evolutionary algorithms in solving large-scale scheduling and resource allocation problems [33]. By evaluating the urgency coefficients of demand points, their model seeks to minimize total cost, delivery time, and survivor dissatisfaction, utilizing a hybrid metaheuristic algorithm that combines discrete particle swarm optimization (DPSO) and Harris hawks optimization (HHO). Emphasizing the dynamic nature of such recovery operations, Li and Zheng (2019) developed a bi-level programming model that integrates post-earthquake road network repair scheduling with relief distribution. Addressing this prerequisite [34], Li and Teo (2019) developed a multi-period bi-level programming model that jointly schedules road network repair work and optimizes relief logistics [35]. By employing a hybrid steady-state parallel genetic algorithm (HSSPGA), their approach effectively balances the recovery of road network accessibility in the upper level with the fairness and efficiency of relief allocation in the lower level. Building upon this foundation, Li, Ma, and Teo (2020) further formulated a nonlinear programming model that intricately integrates logistics support scheduling with the repair crew scheduling and routing problem (RCSRP), utilizing an intertwined two-stage heuristic algorithm to ensure that critical routes are restored rapidly to facilitate subsequent relief efforts [36].

To meet the stringent time constraints inherent in urban emergency response, Li et al. (2024) proposed an integrated emergency vehicle scheduling model operating within a bounded time horizon—thereby extending the literature on time-sensitive dispatch [37]. In congested urban environments, Li et al. (2024) formulated a bi-level optimization model that explicitly captures the interdependence between evacuation routing decisions and rescue vehicle dispatch [38]. Methodological advances continue to broaden the scope of emergency logistics research: Li et al. (2025) proposed a two-stage robust optimization model for emergency service facility location-allocation under demand uncertainty [39]. Ozdemir et al. (2026) developed a two-stage volunteer assignment model for post-disaster search and rescue operations, providing additional insights into rescue personnel allocation under disaster scenarios.

In contemporary search-and-rescue operations, emerging technologies are increasingly incorporated into decision-support models: for example [40], Liu et al. (2026) improved emergency response efficiency in complex post-disaster industrial zones by optimizing the coordinated deployment of drone swarms [41]. Further advancing the application of unmanned aerial vehicles (UAVs) in emergency logistics, Cao et al. (2025) addressed the dual challenges of environmental dynamics and demand uncertainty in disaster relief material distribution [42]. Xiong et al. (2025) further investigated collaborative coverage path planning for UAV swarms in multi-region post-disaster assessment tasks, improving the efficiency of large-scale disaster reconnaissance [43]. They formulated a robust optimization model for multi-UAV task allocation and path planning, which is solved using an improved genetic algorithm and an improved artificial fish swarm algorithm to ensure reliable supply delivery even under maximum demand fluctuations. Complementing this technological focus, Luo et al. (2022) developed an emergency station location model that explicitly balances service efficiency and equity, aiming to reduce urban–rural disparities in emergency medical accessibility [44]. Collectively, these studies demonstrate the evolution of emergency transportation strategies from isolated operational decisions toward integrated and system-level optimization frameworks. However, the interaction between rescue dispatch and subsequent medical treatment remains insufficiently explored [45].

2.2. Dynamic allocation of medical emergency resources

Efficient allocation of medical resources plays a pivotal role in improving the effectiveness of collaborative post-disaster rescue operations. To mitigate supply–demand mismatches during emergencies, Wan et al. (2020) developed a hospital-level resource allocation model based on a Markov decision process framework. Ni and Zhao (2015) conceptualized resource distribution as a time-sensitive, dynamic process incorporating delay penalties [46], whereas Pan et al. (2019) embedded injury progression dynamics into a dynamic programming model to optimize treatment scheduling [47]. Extending this focus on dynamic patient health statuses to pre-hospital transportation, Rabbani et al. (2022) proposed a mixed-integer linear programming (MILP) model for ambulance routing in disaster response [48]. By explicitly accounting for variable patient conditions, their framework utilizes NSGA-II and MOPSO algorithms to minimize both the latest service completion time and the number of patients whose health deteriorates due to untimely medical aid. Du (2024) presented a data-driven decision-support framework that integrates epidemic detection and adaptive medical resource allocation [49]. Zhang et al. (2021) proposed a two-stage stochastic programming approach for allocating limited medical reserve resources under demand and operational uncertainties [50]; similarly, Chen et al. (2016) applied a two-stage optimization methodology to determine minimum staffing levels and schedules under uncertainty [51]. Stefanini et al. (2020) advanced a data-driven, process mining–based methodology to support health-service resource planning—demonstrating how real-world operational data can inform capacity planning and staffing decisions within complex, multi-step care pathways [52].

Yu et al. (2019) and Ho et al. (2019) independently developed rollout-based dynamic programming algorithms to enhance computational tractability in humanitarian logistics and health system management, respectively [53,54]. Yu et al. (2020) employed Timed Colored Petri Nets (TCPNs) to model multi-resource, multi-activity hospital operations [55]. Boostani et al. (2021) extended this line of research by developing a sustainable humanitarian relief logistics model applicable to both pre- and post-disaster contexts, jointly minimizing operational costs and maximizing social welfare [56]. Cai and Ye (2026) investigated time-constrained post-pandemic distribution planning and integrated Gini coefficient–based equity considerations into allocation–routing decisions; their approach, solved via a two-stage heuristic and validated using a real-world case study in Shanghai, ensures fair and timely resource delivery [57].

2.3. Operating room scheduling and emergency optimization

Operating room (OR) scheduling is widely recognized as one of the most resource-intensive and operationally critical functions within hospitals. Batista et al. (2020) proposed a bi-objective stochastic optimization model to balance operational costs and resource utilization efficiency [58]. Tang and Wang (2015) proposed an adjustable robust optimization framework for allocating elective and emergency surgery capacity under demand uncertainty [59]. Addis et al. (2024) analyzed the impact of varying robustness levels on OR scheduling performance through a cardinality-constrained robust optimization model [60].

Chikhi and Djehiche (2024) formulated a three-stage flow-shop scheduling model that explicitly incorporates patient transportation and multiple interdependent resources [61]. Wang et al. (2021) explored cross-departmental resource-sharing strategies to enhance the efficiency of elective surgery scheduling [62]. Bektur and Aslan (2024) modeled anesthesia teams as flexible, cooperative resources and optimized their assignment using an artificial bee colony algorithm [63].

To address the dynamic and uncertain nature of emergency conditions, Tong et al. (2019) proposed a multi-objective optimization model for integrated scheduling of elective and emergency surgeries [64]. Complementing this, Feng et al. (2017) developed a stochastic multi-objective simulation-optimization algorithm that hybridizes the NSGA-II evolutionary algorithm with the multi-objective optimal computing budget allocation (MOCBA) method [65]. Akbarzadeh and Maenhout (2024) proposed a two-layer heuristic method integrating evolutionary search and machine learning prediction to enhance computational efficiency [66].

2.4. Research gaps and analysis

Despite substantial progress in emergency logistics, medical resource allocation, and operating-room scheduling, several important research gaps remain.

(1) Most existing studies investigate pre-hospital emergency dispatch and in-hospital medical scheduling separately. Limited attention has been devoted to integrated decision-making frameworks that explicitly capture the interactions among rescue dispatch, traffic control, casualty transportation, and downstream medical resource allocation.

(2) Existing optimization models generally focus on resource availability and operational efficiency while paying insufficient attention to human factors that influence medical-service performance under emergency conditions. In particular, learning effects, fatigue effects, and bounded rationality may significantly affect treatment outcomes and resource utilization. Recent reviews have emphasized the need for more behaviorally informed and practically deployable decision-support models in humanitarian operations.

Table 1 provides a comparative summary of the most relevant studies and reveals that few existing works simultaneously consider emergency dispatch, traffic control, medical resource allocation, and human behavioral factors within a unified decision-making framework. To address these gaps, this paper develops (i) a traffic-control-aware collaborative dispatch model that jointly optimizes fire-service deployment, hospital selection, and emergency traffic management, and (ii) a dynamic medical-resource allocation model that explicitly incorporates learning effects, fatigue effects, and injury severity. Together, these components form an integrated two-stage framework for improving the coordination and effectiveness of urban emergency response operations.

3. Problem description and model formulation

3.1. Problem description

When a major disaster occurs at a location within a city, the emergency department coordinates on-site rescue operations. Fire and medical personnel must arrive promptly to initiate life-saving interventions. Concurrently, the traffic management authority may implement limited signal-priority traffic control measures at selected intersections to facilitate rapid emergency vehicle movement within the disaster-response area. Upon arrival, first responders triage and stabilize the injured, who are then transported to designated hospitals for definitive care. Consequently, the end-to-end rescue process comprises two interdependent stages. Due to evolving information availability during disaster response, the coupling between the two stages is intentionally modeled as a progressive decision process. In the initial emergency stage, hospital selection primarily focuses on rapid accessibility and transportation capability, while detailed treatment-resource allocation is performed after casualty stabilization and more reliable medical information becomes available. In the first stage, nearby fire units and receiving hospitals are jointly allocated based on the incident's geographic location and injury severity. Considering that fire engines and ambulances are dispatched simultaneously from multiple locations, and that emergency operations can only be effectively initiated after all critical rescue resources arrive, real-time traffic control conditions are explicitly incorporated to minimize the response completion time, defined as the latest arrival time among all dispatched fire and medical rescue resources. In the second stage, after completing the on-site basic rescue, injured patients are transported to hospitals according to injury severity, with medical resources dynamically allocated to minimize deterioration costs within the shortest possible treatment horizon.

It is assumed that there is a set of fire services F around the accident site, indexed by $f = \{1,2,3,4,...,f\}, f \in F$, and a set of hospitals H, indexed by $h = \{1,2,3,4,...,h\}, h \in H$. Let integer decision variables x_f and m_h represent the number of fire engines dispatched from the fire service f and the number of ambulances dispatched from the hospital h, respectively. The total demands for fire engines and ambulances required at the disaster site are denoted as $D_F = 20$ and $D_H = 20$, respectively.

Furthermore, let I denote the set of traffic lights encountered during the rescue operations, indexed by $i \in \{1,2,\ldots,|I|\}$. The base travel times from each fire service and hospital to the rescue site are defined as t_f and t_h, respectively. To determine the traffic control strategy, a binary decision variable n_i is introduced for each traffic light $i \in I$, where $n_i = 0$ indicates that traffic control is imposed at intersection i (allowing rapid passage without delay), and $n_i = 1$ indicates normal traffic light operation. To map the routing connections, binary parameters δ_{fi} and γ_{hi} are defined: $\delta_{fi} = 1$ (or $\gamma_{hi} = 1$) if the route from the fire service f (or hospital h) passes through traffic light i, and 0 otherwise.

Table 1. Summary of related literature.

Reference	Domain	Model	MA	TC	MR/OR	UB	Method	Tool
O'Brien et al. (2020)	Emergency Dispatch (ED)	Conceptual framework (DSA)	√	–	–	–	Conceptual	–
Gooding et al. (2022)	ED	Policy synthesis	√	–	–	–	Qualitative	–
Every-Palmer et al. (2023)	ED	Quasi-experimental (QE)	√	–	–	–	Statistical	–
Su et al. (2023)	Traffic control (TC)	Simulation + MARL	√	√	–	√	MARL	Python
Cao et al. (2022)	TC	Control model	–	√	–	–	Control opt.	MATLAB
Hao et al. (2024)	TC	Systematic review (SR)	–	√	–	–	Review	–
Fiedrich et al. (2000)	SAR	Dynamic optimization model	√	–	–	√	Heuristics	–
Caunhye et al. (2012)	EL	Literature review	–	–	–	–	Review	–
Wu et al. (2021)	Traffic allocation	Optimization framework	√	√	–	–	Optimization	MATLAB
Qin et al. (2018)	Traffic allocation	Rel.-constr. model	–	√	–	√	GA	MATLAB
Liu et al. (2022)	EL	Routing optimization	–	–	–	–	MVO+DE	–
Caunhye et al. (2016)	EL	Location-routing model	√	–	–	√	Two-stage SP	CPLEX
Hu et al. (2025)	EL	Robust location-routing	√	–	–	√	Robust opt	Python
Yan et al. (2023)	EL/LRP	Multi-objective LRP model	–	–	–	–	Hybrid DPSO	
Li & Zheng (2019)	Relief distribution	Bi-level programming model	–	–	–	–	SSHGA	MATLAB
Li & Teo (2019)	Relief logistics	Multi-period bi-level programming model	–	–	–	–	HSSPGA	Open-MPI+Fortran
Li et al. (2020)	EL	Nonlinear programming model	–	–	–	–	ITSHA	MATLAB+CPLEX
Li et al. (2024a)	ED	Integrated scheduling model	√	–	–	√	NSGA-II	MATLAB
Li et al. (2024b)	Traffic evacuation	Bi-level model	√	√	–	√	Bi-level + GA	–

Continued on next page

Reference	Domain	Model	MA	TC	MR/OR	UB	Method	Tool
Dou et al. (2023)	Traffic evacuation	MO model	–	√	–	√	MO opt.	–
He et al. (2015)	Traffic evacuation	Dynamic MILP	–	√	–	–	Benders	CPLEX
Liu et al. (2024)	Traffic evacuation	Dist. bi-level	√	√	–	–	Dist. alg.	Gurobi
Liu et al. (2026)	ED	CVRP-DPA & R-PDP models	√	–	–	–	Improved WOA	–
Cao et al. (2025)	Emergency rescue	Robust optimization model	√	–	–	–	GA&IAFSA	Gurobi
Ozdemir et al. (2026)	SAR	Two-stage assignment model	√	–	–	√	Two-stage MIP	GAMS/CPLEX
Valaei et al. (2026)	SAR	Robust location-allocation	√	–	–	√	Robust opt	Python/Gurobi
Xiong et al. (2025)	SAR/ED	Collaborative CPP	√	–	–	√	Set-based PSO	MATLAB
Rauchecker et al. (2019)	Emerg. Logistics (EL)	Binary LP	–	√	–	–	IP	–
Shiri et al. (2020)	EL	Robust MIP	–	√	–	√	MIP +heure.	CPLEX
Tirkolaee et al. (2020)	EL	Robust MILP	–	√	–	√	RO	GAMS
Shahparvari et al. (2021)	EL	MO model	√	√	–	–	GA	GAMS
Tang et al. (2022)	EL	MO model	–	√	–	–	MO opt.	–
Sperlin et al. (2022)	EL	MO MILP	–	√	–	–	MILP	–
Wan et al. (2020)	Hosp. Emerg.	MDP	–	–	√	√	MDP + PSO	MATLAB
Ni et al. (2015)	Med. Allocation (MR)	Dynamic model	–	–	√	–	Dyn. opt.	–
Pan et al. (2019)	MR	DP	–	–	√	√	DP	–
Rabbani et al. (2022)	Disaster response	MILP	–	–	√	–	NSGA-II	–
Zhang et al. (2021)	MR	Two-stage SP	√	–	√	√	SP	Gurobi
Yu et al. (2019)	Hum. Logistics (HL)	ADP	√	√	√	√	Rollout	MATLAB

Continued on next page

Reference	Domain	Model	MA	TC	MR/OR	UB	Method	Tool
Ho et al. (2019)	MR	Multi-fidelity ADP	–	–	√	√	ADP	MATLAB
Yu et al. (2020)	MR	TCPN simulation	–	–	√	–	TCPN	CPN Tools
Boostani et al. (2021)	HL	Hybrid SP	–	√	√	√	Hybrid SP	–
Batista et al. (2020)	OR scheduling (OR)	Two-stage SP	–	–	√	√	SP	–
Feng et al. (2017)	ED resource alloc.	Sim-based opt.	–	–	√	√	NSGA-II	MATLAB
Tang & Wang (2015)	OR	Adjustable RO	–	–	√	√	RO	CPLEX
Akbarzadeh & Maenhout (2024)	OR	Heuristic + ML	–	–	√	–	Heuristic	Python
Bektur & Aslan (2024)	OR	MILP + metaheur.	–	–	√	–	ABC	MATLAB
Chikhi & Djehiche (2024)	OR	3-stage MIP	–	–	√	–	MIP	CPLEX
Addis et al. (2024)	OR	Cardinality RO	–	–	√	√	RO	Gurobi
Wang et al. (2021)	OR	MIP sharing	√	–	√	–	MIP	Gurobi
Tong et al. (2019)	OR	MO opt.	–	–	√	–	MO opt.	–
This paper	OR	Two-stage SP+ Dynamic model	√	√	√	√	GA+DP	Python+ MATLAB

*Note: Abbreviations are defined at their first appearance.

After the emergency, H hospitals participate in the rescue, and each hospital has a homomorphic surgical center equipped with $\mathbb{N}_0$ operating rooms. These operating rooms are classified based on air cleanliness by particle concentration, following the International Organization for Standardization (ISO) 14644-1 standard [67]. The total operating rooms ($\mathbb{N}_0$) are divided into two types to accommodate different levels of patient acuity and surgical risk:

(1) $\mathbb{N}_{01}$ ISO Class 7 Operating Rooms: These are standard operating rooms (equivalent to the former US FED-STD-209E Class 10,000) designated for general surgery and patients with moderate injuries.

(2) $\mathbb{N}_{02}$ ISO Class 6 Operating Rooms: These are ultra-clean operating rooms (equivalent to the former Class 1000) providing a significantly higher level of air cleanliness. They are reserved for high-risk procedures and patients with severe trauma (e.g., those requiring implants or at high risk of infection), where minimizing airborne contaminants is critical to prevent surgical site infections (SSIs) [68]. The total capacity of the surgical center is $\mathbb{N}_{01} + \mathbb{N}_{02} = \mathbb{N}_0$.

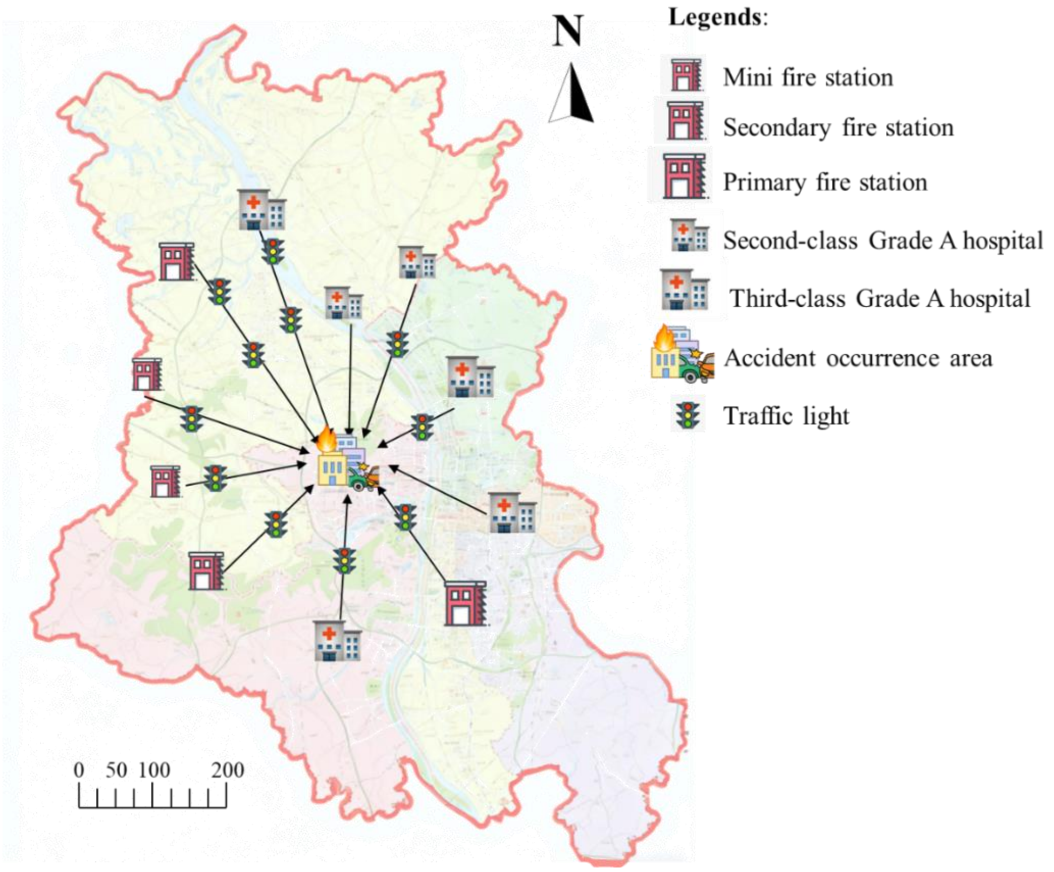

Figure 2. Schematic diagram of emergency collaborative dispatch of search and rescue teams in the first stage.

After the incident, several patients require surgery, classified by operating room level into Thousand-Level and Ten-Thousand-Level, and by injury severity into severe and moderate cases. Each operating room is equipped with a corresponding number of doctors, nurses, and other medical resources based on its specifications.

To minimize rescue time, the model selects the appropriate nearby fire services and hospitals given the rescue requirements.

It determines which fire services and hospitals should be selected under traffic control, how many fire engines and ambulances each should dispatch, and the corresponding optimal rescue routes. With the objective of minimizing personnel loss, the model completes medical treatment considering the threshold fatigue effect and truncated learning effect during surgery, thereby obtaining the minimal deterioration cost for the injured.

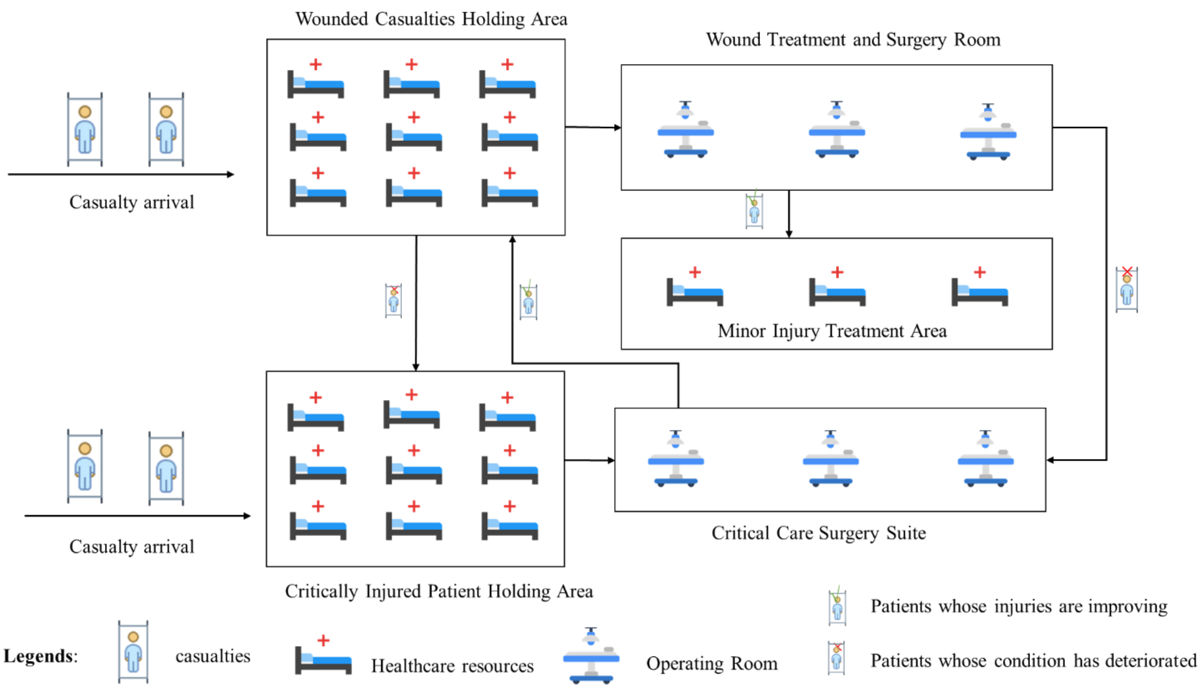

Figure 3. Schematic diagram of the second stage.

Table 2. Parameters and variables of the model.

Index	
F	The set of fire services, $f \in F$
H	The set of hospitals, $h \in H$
I	The set of traffic lights encountered during emergency rescue operations, $i \in I$
K	The set of treatment stages, indexed by $k \in \{1,2,\dots,N\}$
Φ	The set of emergency response phases, indexed by $\Phi \in \{I, II\}$
J	The set of operating room types, indexed by $j \in \{1,2\}$
V	Set of fire-engine types/resources at fire service f
E	Set of ambulances at hospital h
State variables	
$S_1(k)$	The state variable representing the learning effect at stage k
$S_2(k)$	The state variable representing the fatigue effect at stage k
g_{1h}^k, g_{2h}^k	The total number of moderately/severely injured patients waiting for treatment at hospital h at stage k

Continued on next page

Parameters	
D_H	The total number of ambulances required at the rescue site, $D_H = 20$
D_F	The total number of fire engines required at the rescue site, $D_F = 20$
t_f	The travel time from each fire service to the rescue site
t_h	The travel time from each hospital to the rescue site
τ_i	The waiting time at traffic light i
α_h	The learning rate parameter for doctors at hospital h
β_h	The fatigue rate parameter for doctors at hospital h
r_1	The benefit coefficient for a moderately injured patient improving to a minor injury
r_2	The benefit coefficient for a severely injured patient improving to a moderate injury
e_1	The penalty cost associated with ineffective treatment of moderately injured patients
e_2	The penalty cost associated with ineffective treatment of severely injured patients
d_1	The penalty cost per hour of waiting for moderately injured patients
d_2	The penalty cost per hour of waiting for severely injured patients
Decision variables	
x_f	Integer variable: The number of fire engines dispatched from the fire service f
m_h	The number of ambulances dispatched from the hospital h
n_i	1 if traffic control is imposed at the traffic light i, 0 otherwise
δ_{fi}	1 if the route from the fire service f passes the traffic light i, 0 otherwise
γ_{hi}	1 if the route from the hospital h passes traffic light i, 0 otherwise
P_{10}	The probability that a moderately injured person improves to a minor injury
P_{11}	The probability that a moderately injured person's condition remains unchanged
P_{12}	The probability that a moderately injured person deteriorates to a severe injury
P_{21}	The probability that a severely injured person improves to a minor injury
P_{22}	The probability that a severely injured person's condition remains unchanged
P_{23}	The probability that a severely injured person deteriorates to death
a_{1h}^k, a_{2h}^k	Integer variables: The number of moderately/severely injured patients treated at hospital h at stage k
y_{1h}^k, y_{2h}^k	The number of moderately/severely injured patients transported to hospital h at stage k
l_{1h}^k, l_{2h}^k	The number of moderately/severely injured patients who remain in the corresponding operating room for continued treatment at stage k
z_{1h}^k	The number of patients transferred from ISO Class 7 to ISO Class 6 Operating Room
z_{2h}^k	The number of patients transferred from ISO Class 7 to ISO Class 6 Operating Room

3.2. Model assumptions

Assumption a) Traffic-control simplification. To preserve model tractability and applicability across diverse urban environments, traffic control is represented as a simplified emergency signal-priority mechanism rather than a comprehensive urban traffic optimization problem. Emergency vehicles may be granted temporary signal priority at selected intersections, whereas implementation costs, impacts on general traffic, and inter-intersection coordination constraints are not explicitly considered.

Assumption b) Fixed-route rescue. Rescue vehicles are assumed to travel along predetermined shortest-feasible routes identified by existing navigation and emergency-dispatch systems. Consequently, route-selection decisions are beyond the scope of the present study and are not explicitly optimized.

Assumption c) Firefighter–vehicle relationship. Each dispatched fire truck is assumed to be staffed with a standard crew of eight firefighters. Therefore, firefighter demand is implicitly satisfied through fire-truck dispatch decisions and is not modeled separately.

Assumption d) Hospital–ambulance linkage. Each dispatched ambulance is associated with its corresponding receiving hospital. Hospital participation in the first-stage rescue process is represented through ambulance deployment decisions.

Assumption e) Deterministic casualty demand. Casualty demand is assumed to be estimated by the emergency command center based on preliminary incident assessments and is therefore treated as deterministic input during the early stage of emergency response.

Assumption f) Shared hospital resources. Within each hospital, medical personnel and supporting treatment resources are assumed to be flexibly shared among different operating-room categories. Accordingly, resource-allocation decisions are constrained by overall hospital-level treatment capacity rather than ownership of resources by individual operating rooms.

3.3. Model formulation

Based on the problem description, the model is constructed as follows:

First stage:

Objective function:

$$Z_1 = \min T \tag{1}$$

s.t

$$t_f + \sum_{i \in I} \delta_{f_i \tau_i} \left(1 - n_i\right) \le T + M\left(1 - x_f / x_{f\max}\right), \forall f \in F \tag{2}$$

$$t_h + \sum_{i \in I} \gamma_{h_i \tau_i} \left(1 - n_i\right) \le T + M\left(1 - m_h / m_{h\max}\right), \forall h \in H \tag{3}$$

$$\sum_{f \in F} x_f \ge D_F \tag{4}$$

$$\sum_{h \in H} m_h \ge D_H \tag{5}$$

$$0 \le \sum_{f \in F} x_f \le x_{f\max} \tag{6}$$

$$0 \le \sum_{h \in H} m_h \le m_{h\max} \tag{7}$$

Second stage:

Objective function:

$$Z_2 = \max \sum_{k \in K} \sum_{h \in H} \left[c_{1h}^k \left(g_{1h}^k, a_{1h}^k, S_1(k), S_2(k) \right) + c_{2h}^k \left(g_{2h}^k, a_{2h}^k, S_1(k), S_2(k) \right) \right] \tag{8}$$

s.t

$$c_{1h}^k(\cdot) = r_1 a_{1h}^k P_{10}(k \Delta t_{\Phi,1}) - e_1 l_{1h}^{k+1} - d_1 w_{1h}^{k+1} \tag{9}$$

$$c_{2h}^k(\cdot) = r_2 a_{2h}^k P_{21}(k \Delta t_{\Phi,2}) - e_2 l_{2h}^{k+1} - d_2 w_{2h}^{k+1} \tag{10}$$

Objective function (1) minimizes the response completion time in the first-stage emergency rescue process. Since fire engines and ambulances are dispatched simultaneously from multiple origins, the effectiveness of emergency response depends on the arrival of all critical rescue resources. Therefore, the objective is defined as minimizing the latest arrival time among all dispatched fire services and hospitals. Objective function (8) represents that the treatment benefit in the second stage is maximized. Equations (9) and (10) represent the total benefits of ISO Class 7 Operating Room and ISO Class 6 Operating Room in the second stage, respectively. Constraints (2)–(3) ensure that the arrival time of each selected fire service and hospital does not exceed the overall response completion time T. Constraints (4)–(7) guarantee that rescue demand is satisfied and dispatched resources remain within available capacities.

4. Solution algorithm

In this paper, the genetic algorithm is employed in the first stage to solve the multi-rescue team collaborative dispatch problem, while the dynamic programming algorithm is applied in the second stage to address the dynamic allocation of medical resources (see Figure 4).

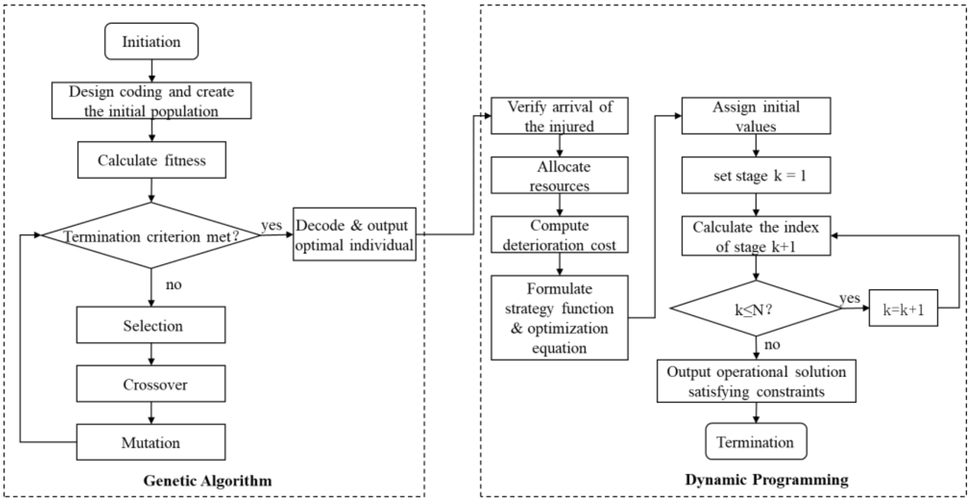

Figure 4. Overall solution algorithm flowchart.

4.1. Genetic algorithm

Genetic algorithms have been widely applied to complex combinatorial optimization problems due to their strong global search capability and computational efficiency. Accordingly, a genetic algorithm (GA) is adopted in this study to solve the coordinated rescue-dispatch problem.

Table 3 summarizes the overall framework of the proposed genetic algorithm. The implementation of the GA begins with the encoding of candidate solutions. Given the specific characteristics of the problem, this study utilizes a segmented encoding strategy. The first segment of the chromosome employs binary encoding, where values of 0 and 1 denote the selection status of a rescue team during emergency dispatch. The second segment represents the quantity of rescue vehicles dispatched by each team and is encoded using integers to express vehicle counts. The third segment corresponds to traffic signals across the entire rescue road network, adopting binary encoding wherein 0 imposes traffic control at an intersection, and 1 indicates unimpeded operation. The best chromosome obtained during the evolutionary process corresponds to the optimal coordinated dispatch scheme for rescue resources.

During decoding, each chromosome is interpreted according to the predefined segmented encoding structure. A chromosome consists of 33 decision variables, including fire-engine dispatch, ambulance allocation, and traffic-light control decisions. Segment 1 (12 integer variables) represents the number of fire engines dispatched from each fire station, where each value is bounded by the corresponding station capacity. Segment 2 (5 integer variables) denotes the number of ambulances dispatched from each hospital, also subject to hospital-specific capacity limits. Segment 3 (16 binary variables) represents the traffic-light control status along the rescue road network. A value of 0 indicates that signal-priority control is activated at the corresponding intersection, enabling emergency vehicles to pass with reduced delay, whereas a value of 1 represents normal traffic-light operation. To ensure reproducibility, the GA hyperparameters used in all numerical experiments are explicitly reported. The population size was set to 100, the crossover probability was fixed at 0.8, and the mutation probability was set to 0.3. A uniform crossover strategy and random perturbation mutation operator were employed. Parent chromosomes were selected using a tournament-selection mechanism with a tournament size of three. The stopping criterion was defined as a maximum of 1000 iterations. Furthermore, to ensure reproducibility and reduce stochastic variability across runs, the random seed for both the NumPy and Python random generators was fixed at 42.

The three chromosome segments are subsequently integrated to generate a feasible rescue-dispatch plan, including resource selection, vehicle allocation, and traffic-control decisions.

Table 3. Multi-team coordinated dispatch algorithm.

Algorithm 1: Genetic algorithm

Input: Coding scheme parameters, population size, termination criteria
Output: Optimal solution
Initialize population P using the coding scheme
Evaluate fitness of each individual in P
While termination criteria are not met do
  Select parent individuals from P based on fitness
  Generate offspring via crossover on selected parents
  Apply mutation to offspring with predefined probability
  Update P by replacing less fit individuals with offspring
  Re-evaluate fitness of updated P
End while
Decode the fittest individual in P and return as optimal solution

4.2. Dynamic programming for resource allocation

4.2.1. Deterioration cost calculation

Following a disaster event, such as an earthquake, injured individuals are progressively transported to hospitals by ambulance for emergency treatment. During transportation, the START triage protocol is employed to classify patients according to injury severity, following the principle of prioritizing life-saving interventions and the treatment of critically injured patients. In this classification method, patients are divided into four categories: deceased or untreatable (black), severe injuries (red), moderate injuries (yellow), and minor injuries, which are represented by states 3, 2, 1, and 0, respectively. Patients with severe, moderate, and minor injuries are transported to hospitals for treatment. Because patients with different injury severities require different levels of medical resources, three categories of operating rooms are designated to improve treatment efficiency and resource utilization. Severely injured patients are assigned to the ISO Class 6 Operating Room, moderately injured patients to the ISO Class 7 Operating Room, and lightly injured patients to the ISO Class 8 Operating Room for treatment. As treatment progresses, the conditions of the wounded change; for example, patients treated in the ISO Class 6 Operating Room who improve to state 2 are transferred to the ISO Class 7 Operating Room. When the wounded have not yet received treatment, the survival rates of the two categories of injuries are shown in Figure 5. It can be seen that as time progresses, the survival rates of both types of injuries gradually decrease, and the rate of decline slows over time. As patient conditions deteriorate and survival probabilities decline over time, treatment outcomes may differ substantially depending on hospital arrival time. After the injured arrive at the hospital and receive treatment, the transition matrix of injury states is as follows:

$$\Phi = \begin{vmatrix} P_{00} & P_{01} & P_{02} & P_{03} \\ P_{10} & P_{11} & P_{12} & P_{13} \\ P_{20} & P_{21} & P_{22} & P_{23} \\ P_{30} & P_{31} & P_{32} & P_{33} \end{vmatrix} \tag{11}$$

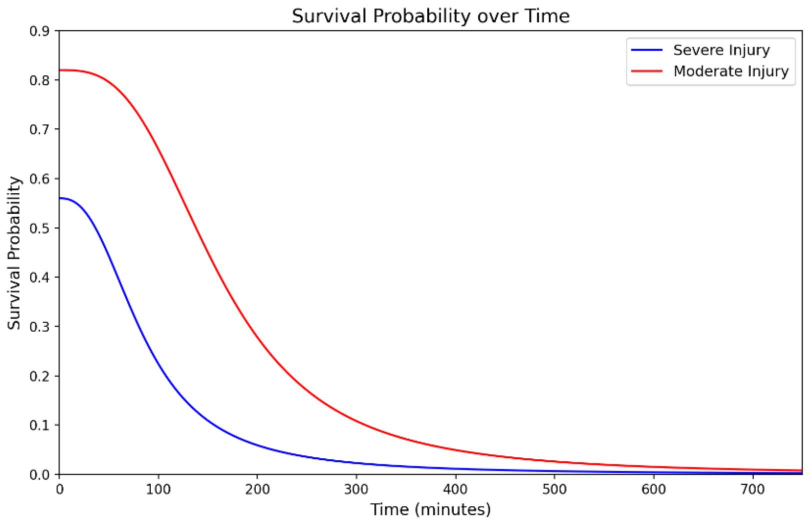

Figure 5. Survival function.

Since the stable states 0 and 3 do not transition to other states, this paper focuses on the potential deterioration of severely and moderately injured patients during the time it takes to reach the hospital, as well as on the transitions of injury states during treatment. It is assumed that within the effective treatment period, the condition of treated patients will not worsen to a more severe state, and that their condition will gradually improve after receiving medical care. Therefore, only transitions between adjacent states or maintenance of the current state are considered. However, during transportation to the hospital, the condition of patients may deteriorate; thus, the injury state transition matrix is revised as follows:

$$\Phi = \begin{vmatrix} 0 & 0 & 0 & 0 \\ P_{10}(\mathrm{t}) & P_{11}(\mathrm{t}) & P_{12}(\mathrm{t}) & 0 \\ 0 & P_{21}(\mathrm{t}) & P_{22}(\mathrm{t}) & P_{23}(t) \\ 0 & 0 & 0 & 0 \end{vmatrix} \tag{12}$$

As time progresses, patients whose conditions continuously deteriorate exhibit similar implicit semi-Markov characteristics in their post-treatment injury-state transitions. Therefore, in modeling the injury transitions, this paper introduces a multiplicative deterioration factor. Based on this, the transition probability of patients treated in the ISO Class 7 Operating Room is derived as follows:

$$P_{10}(\mathrm{k}\Delta \mathrm{t}_1) = p_{10}(k-1)(1+\eta) = p_{10}(0)(1+\eta)^k \tag{13}$$

$$P_{12}(\mathrm{k}\Delta \mathrm{t}_1) = p_{10}(k-1)(1-\eta) = p_{10}(0)(1-\eta)^k \tag{14}$$

$$P_{11}(t) = 1 - p_{10}(t) - p_{12}(t) \tag{15}$$

Similarly, the injury-state transition probabilities for patients treated in the ISO Class 6 Operating Room are as follows:

$$P_{23}(k\Delta t_2) = p_{20}(k-1)(1-\theta) = p_{21}(0)(1-\theta)^k \tag{16}$$

$$P_{21}(k\Delta t_2) = p_{21}(k-1)(1+\theta) = p_{21}(0)(1+\theta)^k \tag{17}$$

$$P_{22}(t) = 1 - p_{23}(t) - p_{21}(t) \tag{18}$$

To ensure mathematical validity, the transition probabilities are dynamically bounded and normalized at each decision stage. The updated expressions in Equations (13) and (18) characterize the transition tendency under physician learning and fatigue effects, while the final transition probabilities are constrained to satisfy

$$0 \le P_{ij}\left(k\right) \le 1 \tag{19}$$

and

$$\sum_j P_{ij}\left(k\right) = 1. \tag{20}$$

The detailed bounded updating mechanism is presented in Appendix A.6. Therefore, infeasible transition probabilities (e.g., probabilities exceeding 1 or becoming negative) do not occur during model execution.

Considering the effects of framing, learning, and fatigue on the overall rescue system, the settings of the learning and fatigue effects are defined as follows:

(1) Learning effect variable

Let $S_1(k)$ denote the state variable representing the learning effect factor for the medical team at hospital $h \in H$ during stage $k \in K$. The learning effect factor increases with the cumulative number of treated patients, reflecting improvements in physician experience, procedural familiarity, and team coordination during prolonged rescue operations.

(2) Fatigue effect variable

Let S_2 denote the state variable representing the fatigue effect factor for the medical team at hospital $h \in H$ during stage $k \in K$. The fatigue effect factor increases with continuous working time, representing the accumulation of physical and cognitive fatigue that may reduce treatment efficiency and increase operational risk. When S_2 reaches the threshold $S_2^{\max}$ (the maximum allowable continuous working time), the medical team must rest for ρ minutes. During the rest period, the team does not participate in treatment, and the fatigue effect is reset after rest as they recover energy. It should be noted that $S_2(k)$ represents the fatigue level of medical staff rather than effective working capability. Therefore, an increase in fatigue reduces treatment effectiveness, and the probability of patient improvement is modeled through $1-S_2(k)$. Considering both learning and fatigue effects, the probability that a patient's condition improves after treatment in the ISO Class 7 Operating Room is:

$$P_{10}(k\Delta t_1) = p_{10}(0)\cdot(1+\eta)^k \cdot S_1(k)\cdot(1-S_2(k)) \tag{21}$$

Similarly, the probability that the condition of patients treated in the ISO Class 6 Operating Room improves is:

$$P_{21}(k\Delta t_2) = p_{21}(0)\cdot(1+\theta)^k \cdot S_1(k)\cdot(1-S_2(k)) \tag{22}$$

(3) Calculation of the learning effect factor

The learning effect factor $S_1(k)$ is dynamically determined based on the cumulative number of patients treated by the doctors at hospital h. Let $N_h(k)$ denote the cumulative number of patients treated at hospital h prior to stage k. Then, the learning effect factor can be expressed as:

$$S_1(k) = 1+\alpha_h \ln(1+N_h(k)) \tag{23}$$

Here, α_h represents the learning rate parameter defined in Table 2, indicating the specific rate at which doctors at the hospital h improve their rescue efficiency through experience.

(4) Calculation of the fatigue effect factor

The fatigue effect factor $S_2(k)$ is calculated based on the doctors' continuous working time during the emergency response. Let $T_h(k)$ denote the continuous working time of the medical team at hospital before stage k. Then, the fatigue effect factor is formulated as:

$$S_2(k) = 1-e^{-\beta_h T_h(k)} \tag{24}$$

Here, β_h represents the fatigue rate parameter defined in Table 2, indicating the rate at which doctors' fatigue exponentially increases during prolonged operations.

This formulation reflects the cumulative and nonlinear nature of fatigue, whereby prolonged continuous work leads to accelerating performance degradation. Recent empirical evidence suggests that fatigue not only reduces average performance but also increases the likelihood of extremely low-performance outcomes, highlighting the operational risks associated with sustained workloads [69]. Accordingly, modeling fatigue as a function of continuous working time provides a realistic representation of behavioral deterioration in emergency medical operations.

4.2.2. Patient arrival

The total time from the occurrence of the disaster to the transportation of all casualties to the hospital is denoted as Γ_1 minutes. A decision is made every ΔT_1 minutes, resulting in N_1 decision periods. In certain city emergency scenarios, although medical emergency operations are often difficult to maintain in a steady state, the Poisson distribution can appropriately model the arrival of casualties in cases such as small-scale city road chain accidents with fixed sections or localized residential fires confined to a single community where the fire spread is relatively stable. Unlike the Gamma distribution, which allows time-varying arrival intensities, the Poisson distribution assumes a constant average arrival rate within a specified time interval. According to the findings of Smith et al., in cases such as limited-vehicle chain collisions on specific city road sections where the disaster intensity is relatively low, the process of transporting casualties to hospitals exhibits relatively stable characteristics. During a certain period, the fluctuation in the number of arriving casualties is small, and no sharp dynamic changes occur. Under such conditions, the Poisson distribution can effectively describe the casualty arrival process, with its formula and relevant parameter settings defined as follows. The parameter of the Poisson distribution represents the average arrival rate of casualties per unit time, and its specific value can be determined accurately based on the specific city emergency scenario and statistical data from similar past events. Since in such city emergencies casualties mainly result from single mechanisms such as vehicle collisions or fire burns, and the coordination of city rescue forces and medical resources can proceed at a relatively stable pace, the traditional Poisson distribution law can effectively model casualty arrivals. Consequently, it provides a practical basis for medical-resource allocation and emergency-response planning in the considered urban emergency scenarios.

After all injured patients have arrived at the hospital, the total time required to complete all medical treatments is Γ_2 minutes, during which a decision is made every ΔT_2 minutes, resulting in N_2 decision periods.

4.2.3. Resource allocation

This paper employs a dynamic programming algorithm, considering the situation in which severely injured patients are transferred from the ISO Class 6 operating rooms to the ISO Class 7 operating rooms after treatment. The joint allocation of resources between the ISO Class 6 and the ISO Class 7 operating rooms is analyzed in detail from five aspects: decision epoch, state space, action set, transition probability, and reward.

(1) Decision epoch

The total time allocated for the emergency medical response is denoted as Γ (measured in minutes), which is strictly divided into two sequential phases: the patient arrival phase (Γ_I) and the post-arrival treatment phase (Γ_{II}), such that $\Gamma = \Gamma_I + \Gamma_{II}$. Since all patient treatments must be completed within \$$\Gamma$, this constitutes a finite-horizon decision process.

Let the index $j \in \{1,2\}$ denote the operating room type, where $j=1$ represents the ISO Class 7 Operating Room (for moderately injured patients), and $j=2$ represents the ISO Class 6 Operating Room (for severely injured patients).

During Phase I (Γ_I), casualties are continuously transported to the hospital. Emergency resources for the operating room j are allocated every $\Delta t_{I,j}$ minutes, resulting in a total of $N_{I,j}$ decision epochs for this phase.

During Phase II (Γ_{II}), the casualty arrival process ceases, and decisions are exclusively focused on treating the accumulated patients remaining within the hospital system. In this phase, decisions for the operating room j are made every minute, resulting in $N_{II,j}$ decision epochs.

The time intervals $\Delta t_{I,j}$ and $\Delta t_{II,j}$ are predefined fixed values based on the distinct operational characteristics of each operating room and the specific emergency phase. To align with the overall dynamic programming formulation, let k represent the universal decision stage index mapping across these predefined periods for the joint hospital system.

The hospital possesses various resources such as surgeons, psychologists, nurses, hospital beds, and medications. These medical resources are allocated to different operating rooms according to their specifications, and the demand matrices for operating rooms corresponding to two types of patients are defined as follows:

$$D = (\overrightarrow{d_1}, \overrightarrow{d_2}) \tag{25}$$

$\overrightarrow{d_1}$ represents the medical resources required by a moderately injured patient, and $\overrightarrow{d_2}$ represents the medical resources required by a severely injured patient.

(2) State space

Here, the ISO Class 6 and the ISO Class 7 Operating Room areas of the hospital are regarded as a joint decision-making system. Four groups of patients are treated in the ISO Class 7 operating rooms: moderately injured patients transported to the hospital by ambulance (y_{1h}^k); moderately injured patients who remain in the ISO Class 7 operating rooms for continued treatment (l_{1h}^k); patients transferred from the ISO Class 6 operating rooms to ISO Class 7 operating rooms (z_{1h}^k); and moderately injured patients who were not arranged for treatment in the previous stage (w_{1h}^k). Four groups of patients are treated in ISO Class 6 operating rooms: severely injured patients transported to the hospital by ambulance (y_{2h}^k); severely injured patients who remain in the same operating rooms for continued treatment (l_{2h}^k); patients transferred from the ISO Class 7 operating rooms to the ISO Class 6 operating rooms (z_{2h}^k); and severely injured patients who were not arranged for treatment in the previous stage (w_{2h}^k), as well as those who deteriorate to death (u_{2h}^k).

Let $\Phi \in \{I, II\}$ denote the current response phase. During Phase I (Γ_I), casualties arrive continuously. Based on the discrete stage-mapping approach, the number of newly arriving casualties at the hospital h during stage k is calculated using definite integrals over the respective decision intervals $\Delta t_{I,1}$ and $\Delta t_{I,2}$:

$$y_{1h}^k = \begin{cases} \int_{(k-1)\Delta t_{I,1}}^{k\Delta t_{I,1}} \lambda_1(t)dt, & \text{if in Phase I} \\ 0, & \text{if in Phase II} \end{cases} \tag{26}$$

$$y_{2h}^k = \begin{cases} \int_{(k-1)\Delta t_{I,2}}^{k\Delta t_{I,2}} \lambda_2(t)dt, & \text{if in Phase I} \\ 0, & \text{if in Phase II} \end{cases} \tag{27}$$

Following the implicit semi-Markov deterioration rules, the number of patients transferring between different health states relies on the actual time elapsed, which is explicitly formulated as $(k-1)\Delta t_{\Phi,j}$ for the operating room j at a given phase Φ. The detailed state transitions for the hospital h at stage k are rigorously computed as follows:

$$l_{1h}^k = P_{11}\left((k-1)\Delta t_{\Phi,1}\right) \cdot a_{1h}^{k-1} \tag{28}$$

$$l_{2h}^k = P_{22}\left((k-1)\Delta t_{\Phi,2}\right) \cdot a_{2h}^{k-1} \tag{29}$$

$$z_{1h}^k = P_{21}\left((k-1)\Delta t_{\Phi,2}\right) \cdot a_{2h}^{k-1} \tag{30}$$

$$z_{2h}^k = P_{12}\left((k-1)\Delta t_{\Phi,1}\right) \cdot a_{1h}^{k-1} \tag{31}$$

$$w_{1h}^k = g_{1h}^{k-1} - a_{1h}^{k-1} \tag{32}$$

$$w_{2h}^k = g_{2h}^{k-1} - a_{2h}^{k-1} \tag{33}$$

$$u_h^k = P_{2d}\left((k-1)\Delta t_{\Phi,2}\right) \cdot a_{2h}^{k-1} \tag{34}$$

The patients waiting for treatment before decision-making in the hospital system are regarded as the aggregated system state. Thus, the system states for moderately and severely injured patients at hospital h during stage k are expressed as:

$$g_{1h}^k = y_{1h}^k + l_{1h}^k + z_{1h}^k + w_{1h}^k \tag{35}$$

$$g_{2h}^k = y_{2h}^k + l_{2h}^k + z_{2h}^k + w_{2h}^k \tag{36}$$

(3) Action set

The decision-maker takes two possible actions for the available patients at hospital h : (1) allocate the corresponding resources for immediate treatment (a_{1h}^k, a_{2h}^k) or (2) let the patients wait until the next stage for treatment ($w_{1h}^{k+1}, w_{2h}^{k+1}$). The action set $\mathcal{A}_h^k$ defines the feasible number of patients treated at stage k . To characterize hospital treatment capacity under emergency conditions, a standardized pooled-resource assumption is adopted. Medical resources, including physicians, nurses, beds, and essential surgical support resources, are aggregated into a unified hospital-level capacity indicator. Different operating-room types consume different levels of standardized medical resources. At any decision moment, the resources consumed by the two operating rooms must not exceed the hospital's available capacity R_h :

$$a_{1h}^k d_1 + a_{2h}^k d_2 \le R_h \tag{37}$$

Where d_1 and d_2 denote the standardized resource consumption coefficients required for treating one patient in ISO Class 7 and ISO Class 6 operating rooms, respectively. R_h represents the total available medical resource capacity of hospital (h) during the emergency response period. To maintain computational tractability, all medical resources are represented through a standardized composite resource index.

(4) Transition probability

The transition probability is closely related to the injury transitions between different departments, as shown in the equations, and to the system state representing the number of patients waiting for treatment at the decision moment. The current system state depends not only on the previous stage's decision but also on the number of newly arrived patients and the transfer situation of patients from other departments, as shown in Equations (21) and (22).

(5) Index function

Patients with different injury severities are admitted to different operating rooms and achieve different treatment outcomes according to the injury transition conditions. The system's reward is related to the treatment outcomes of patients. Positive outcomes yield positive rewards, while unchanged or deteriorated conditions incur penalty costs. Considering doctors' learning and fatigue effects, the reward function is expressed as follows:

$$c_{1h}^k(g_{1h}^k, a_{1h}^k, S_1(k), S_2(k)) = r_1 a_{1h}^k P_{10}(k\Delta t_{\Phi,1}) - e_1 l_{1h}^{k+1} - d_1 w_{1h}^{k+1} \tag{38}$$

$$c_{2h}^k(g_{2h}^k, a_{2h}^k, S_1(k), S_2(k)) = r_2 a_{2h}^k P_{21}(k\Delta t_{\Phi,2}) - e_2 l_{2h}^{k+1} - d_2 w_{2h}^{k+1} \tag{39}$$

$$\begin{cases} V_k(s_h^{k+1}) = \max\limits_{a_h^k \in \mathcal{A}_h^k} \left[c_{1h}^k\left(g_{1h}^k, a_{1h}^k, S_1(k), S_2(k)\right) + c_{2h}^k\left(g_{2h}^k, a_{2h}^k, S_1(k), S_2(k)\right) + V_{k-1}(s_h^k) \right] \\ V_0(s_h^1) = 0 \end{cases} \tag{40}$$

Where $V_k(s_h^{k+1})$ represents the optimal cumulative expected reward for hospital h from the initial stage 1 up to the current stage k , resulting in the subsequent state s_h^{k+1} . To strictly satisfy the shared resource capacity constraint defined in Eq. (33), the dynamic programming formulation for moderately and severely injured patients is unified into a joint forward-reaching Bellman optimality equation. The decision variable $a_h^k = (a_{1h}^k, a_{2h}^k)$ represents the joint action taken at stage k , which must belong to the feasible action space $\mathcal{A}_h^k$. $V_{k-1}(s_h^k)$ denotes the optimal cumulative value achieved up to the previous stage $k-1$. The boundary condition is defined at the initial dummy stage 0, where the baseline accumulated reward $V_0(\cdot)$ is strictly 0.

Here, r_1 and r_2 are the benefit coefficients for moderately and severely injured persons improving their conditions, respectively; e_1 and e_2 are the penalty costs for ineffective treatments; and d_1 and d_2 are the hourly waiting penalty costs.

4.2.4. Dynamic programming solution

Based on the forward-reaching approach, let $V_k^{\pi}(s_h^{k+1})$ represent the optimal cumulative total reward under policy π for hospital h from stage 1 up to stage k, resulting in the subsequent state s_h^{k+1}. To satisfy the shared resource constraints, the joint optimality equation is defined as:

$$V_k^*(s_h^{k+1}) = \max_{a_h^k \in \mathcal{A}_h^k}\left[c_{1h}^k(g_{1h}^k, a_{1h}^k, S_1(k), S_2(k)) + c_{2h}^k(g_{2h}^k, a_{2h}^k, S_1(k), S_2(k)) + V_{k-1}^*(s_h^k)\right] \tag{41}$$

Step 1: Initialization. At stage 0, set $V_0(s_h^1) = 0$ and initialize the doctors' learning effect state variable $S_1(0) = 0$ and fatigue effect state variable $S_1(0) = 0$.

Step 2: Let $k = 1$. Adopt the optimal policy $\pi = (V_1^*)$ and compute the index for the second stage $V_1(s_h^2)$.

Step 3: If $k = N$, then $\pi^* = (V_1^*, V_2^*, \ldots, V_N^*)$ is the optimal policy, and the algorithm terminates.

Otherwise, set $k = k + 1$.

Step 4: Determine the action set $\mathcal{A}_h^k$ at stage k and find the action solution $a_h^{k*} = (a_{1h}^k, a_{2h}^k)$ satisfying the given constraints.

Table 4. Dynamic medical resource allocation under the framing effect.

Algorithm 2: Dynamic programming for resource allocation

Input: Injury arrival data, resource constraints, deterioration cost model

Output: Optimal stage-wise resource allocation strategy

```
Validate injury arrival information
Initialize resource pools and deterioration cost parameters
Formulate stage transition function V(k, g_k) and optimization objective V_k^*(s_h^{k+1})
Set initial stage k = 1 and boundary conditions
While k ≤ N (total number of decision stages) do
    Determine feasible joint action space A_h^k satisfying resource capacities
    For each possible state s_h^k at stage k do
        Compute cumulative performance index V_k using Bellman equation
            V_k^*(s_h^{k+1}) = max_{a_h^k ∈ A_h^k} [c_{1h}^k(g_{1h}^k, a_{1h}^k, S_1(k), S_2(k)) + c_{2h}^k(g_{2h}^k, a_{2h}^k, S_1(k), S_2(k)) + V_{k-1}^*(s_h^k)]
        Record optimal action a_h^{k*} that maximizes V_k
    End for
    Set k = k + 1
End while
Extract and return the near-optimal solution consistent with the exact solver strategy
sequence π^* = (a_h^{1*}, a_h^{2*}, ..., a_h^{N*})
```

5. Numerical example and solution analysis

5.1. Numerical example construction and solution

A traffic-accident scenario involving coordinated rescue dispatch and casualty treatment is adopted as the numerical example. After the accident occurs, fire departments and hospitals in three nearby areas participate in the rescue. The disaster site determines that 160 firefighters and 20 fire engines are required for the rescue. The number of injured persons at the scene remains uncertain. A road network is subsequently constructed based on the actual geographical characteristics of the affected area. The locations of fire services and hospitals, road travel times, and signalized intersections are calibrated using real navigation and map information to improve the practical relevance of the case study.

Ordinary fire services are classified into three types: first-level, second-level, and small fire services. According to the City Fire Service Construction Standard GB152-2021, a first-level fire service is equipped with 5–7 fire engines and 30–45 firefighters per shift. A second-level fire service is equipped with 2–4 fire engines and 15–25 firefighters per shift. A small fire service is equipped with 2 fire engines and 15 firefighters per shift.

For computational convenience, this paper assumes that a first-level fire service provides 6 fire engines and 40 firefighters. It assumes that a second-level fire service provides 4 fire engines and 25 firefighters. A small fire service provides 2 fire engines and 15 firefighters per shift.

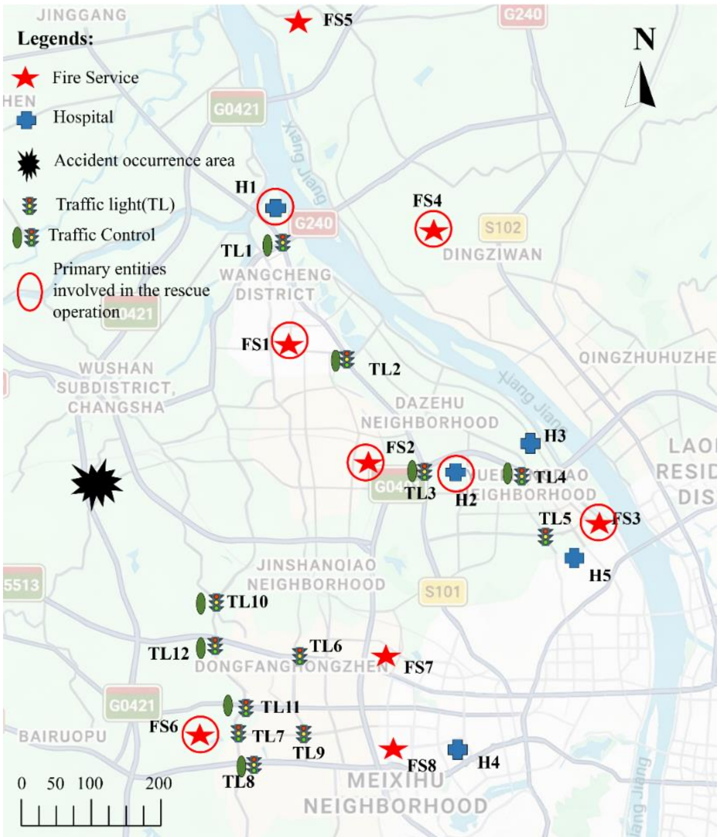

Figure 6. First-stage rescue results.

Table 5. Fire service information.

Fire service	Type	Number of fire engines	Travel time (min)	Traffic lights passed
Service 1	Primary fire service	6	11	-
Service 2	Small fire service	2	14	L10, L12
Service 3	Secondary fire service	4	18	L4, L5, L6, L3, L12
Service 4	Small fire service	3	25	L1
Service 5	Small fire service	3	37	L1
Service 6	Primary fire service	5	26	L11, L12
Service 7	Primary fire service	5	31	L12, L11
Service 8	Secondary fire service	4	30	L6, L12

Table 6. Hospital information.

Hospital	Type	Number of ambulances	Travel time (min)	Traffic lights passed
Hospital 1	Grade II Level A Hospital	10	15	L1
Hospital 2	Grade III Level A Hospital	10	18	L3
Hospital 3	Grade III Level A Hospital	15	27	L3, L6, L12
Hospital 4	Grade III Level A Hospital	15	50	L7, L8, L9, L11
Hospital 5	Grade III Level A Hospital	15	58	L5, L6

The proposed GA is applied to solve the first-stage coordinated dispatch problem and determine the participating fire stations and hospitals. The latest arrival time is calculated as follows: $T = 26.00\,\text{min}$. Based on the optimized dispatch strategy, the response times of participating rescue units range from 11.00 to 26.00 min, with a maximum response completion time (latest arrival time) of 26.00 min. Specifically, 42.9% of dispatched rescue resources arrive within 15 min, 71.4% arrive within 20 min, and 85.7% complete arrival within 25 min.

Importantly, all dispatched rescue resources complete arrival within 26 min, which remains below the 30-min emergency-response horizon commonly regarded as operationally acceptable for large-scale disaster scenarios. Although several dispatched units exceed the conventional 15-min emergency-response benchmark, this result is reasonable in large-scale disaster scenarios requiring simultaneous mobilization of multiple rescue facilities. These findings highlight the importance of maintaining adequate emergency-service coverage and geographically distributed infrastructure to enhance response resilience during large-scale urban emergencies [70,71].

Table 7. Fire department dispatch results.

	Fire service ID	Number of dispatched vehicles	Arrival time (min)
Fire department dispatch results	Service 1	6	11
	Service 2	2	14
	Service 3	4	19.17
	Service 4	3	25
	Service 6	5	26

Table 8. Hospital dispatch results.

	Hospital ID	Number of dispatched vehicles	Arrival time (min)
Hospital dispatch results	Hospital 1	10	15
	Hospital 2	10	18

Table 9. Traffic light control results.

Traffic light control results	Traffic light 1	Traffic light 2	Traffic light 3	Traffic light 4
	Controlled	Controlled	Controlled	Controlled
	Traffic light 5	Traffic light 6	Traffic light 7	Traffic light 8
	No traffic control	No traffic control	No traffic control	Controlled
	Traffic light 9	Traffic light 10	Traffic light 11	Traffic light 12
	No traffic control	Controlled	Controlled	Controlled

To validate the applicability and effectiveness of the proposed genetic algorithm (GA) for the first-stage coordinated rescue dispatch problem, comparative experiments were conducted against the ant colony optimization (ACO) algorithm under identical datasets, constraints, and iteration settings. In addition, the Gurobi exact solver was introduced as an optimization benchmark to verify the quality of heuristic solutions. Performance comparison results are shown in Figure 7 and summarized in Table 10.

The results indicate that the proposed GA achieves superior performance in terms of both solution quality and computational efficiency.

a) Solution quality: Under the revised min–max objective, the first-stage model seeks to minimize the response completion time, defined as the latest arrival time among all dispatched emergency resources. The GA obtained a best response completion time of 26.00 min, which matches the optimal objective value verified by the Gurobi exact solver. In contrast, the ACO algorithm converged to a suboptimal solution with a response completion time of 27.00 min, suggesting a greater tendency toward premature convergence when handling mixed discrete decision variables associated with rescue-resource allocation and traffic-control decisions. Although the dispatch plans generated by the GA and Gurobi differ slightly in terms of fire-station assignments and traffic-control configurations, both approaches achieve the same objective value of 26.00 min. This finding indicates the existence of multiple equivalent optimal solutions under the min–max objective.

This equivalence can be attributed to the bottleneck nature of the min–max objective. Because the objective value is determined solely by the latest arrival time among all active rescue resources, only the slowest dispatched rescue unit directly influences the optimization outcome. Consequently, traffic-control decisions that do not affect the bottleneck route, as well as route segments associated with inactive rescue stations, become non-binding and may vary without altering the final response completion time.

b) Computational efficiency: Rapid decision-making is critical in urban emergency-response operations. The proposed GA identified the optimal-quality dispatch plan within 5.14 s, whereas the ACO algorithm required 78.89 s, representing a substantial reduction in computational effort. Although the Gurobi solver obtained the exact optimal solution most rapidly (0.01 s) for the present case study, exact optimization may become increasingly difficult when the model is extended to larger transportation networks, stochastic demand environments, dynamic routing decisions, or stronger inter-stage interactions. Therefore, the proposed GA offers a practical compromise between solution quality, computational efficiency, and scalability.

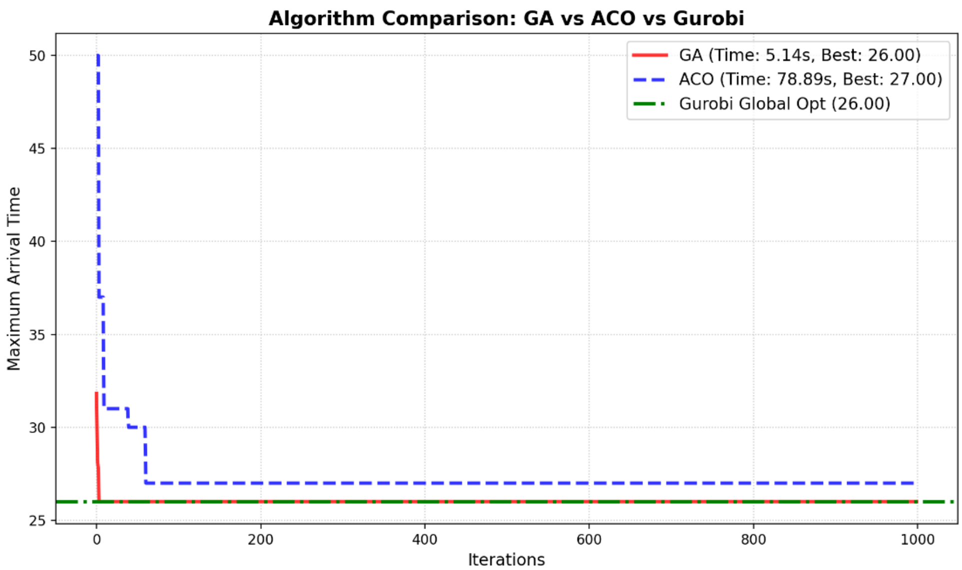

Figure 7. Convergence performance comparison between the GA and ACO for the first-stage coordinated dispatch problem.

Table 10. Algorithmic performance comparison.

Algorithm	Best objective value (min)	Computation time (s)	Convergence characteristics
GA	26.00	5.14	Reaches Gurobi-verified optimal objective
ACO	27.00	78.89	Premature convergence to the suboptimal solution
Gurobi	26.00	0.01	Exact optimal solution

As shown in Table 11, the solutions obtained by GA and Gurobi are highly consistent in terms of rescue-resource allocation, particularly in hospital dispatch decisions, while slight differences exist in selected fire-station quantities and traffic-control strategies. Despite these discrepancies, both approaches achieve the same minimum response completion time (26.00 min), indicating the presence of multiple equivalent optimal solutions.

This phenomenon is primarily attributed to the min–max optimization objective, which exhibits a bottleneck effect. Since the objective is determined exclusively by the latest arrival time among all active rescue resources, variations in traffic-light control that do not influence the bottleneck rescue path do not alter the final objective value. Moreover, traffic lights associated with inactive rescue stations become effectively non-binding in the optimization process. Consequently, different traffic-control configurations may lead to the same optimal response completion time. By contrast, the ACO algorithm produces substantially different dispatch and traffic-control decisions, leading to a longer response completion time (27.00 min), which further demonstrates the effectiveness of the proposed GA in solving the first-stage coordinated rescue dispatch problem.

Table 11. Detailed optimal dispatch results of different algorithms.

Algorithm	Objective	Fire station dispatch array (FS1−FS12)	Hospital dispatch array (H1−H5)	Traffic light array
GA	26.00	[6, 2, 4, 3, 0, 5, 0, 0]	[10, 10, 0, 0, 0]	[0, 0, 0, 0, 1, 1, 1, 0, 1, 0, 0, 0]*
ACO	27.00	[6, 2, 4, 3, 0, 5, 0, 0]	[10, 8, 12, 0, 0]	[0, 0, 0, 0, 0, 0, 0, 0, 0, 0, 0, 0]
Gurobi	26.00	[6, 2, 4, 3, 0, 5, 0, 0]	[10, 10, 0, 0, 0]	[0, 0, 0, 0, 0, 0, 0, 0, 0, 0, 0, 0]

*Notes: To facilitate computation, a value of 0 denotes the presence of traffic control, while a value of 1 denotes the absence of traffic control.

To further evaluate the effectiveness of the proposed traffic-control strategy, comparative experiments were conducted under three scenarios: no traffic control, full traffic control, and optimized adaptive traffic control. The comparison results are summarized in Table 12. The results indicate that the no-control scenario produces the worst system performance, with a response completion time of 28 min. In contrast, both the full-control and optimized adaptive-control strategies reduce the latest arrival time to 26.00 min, representing a 7.1% improvement over the no-control scenario.

More importantly, the proposed adaptive strategy achieves the same response-completion performance as the full-control policy without requiring system-wide signal intervention. This result suggests that large-scale traffic control is not always necessary during emergency response operations. Instead, selectively coordinated signal-priority interventions can achieve comparable rescue efficiency while potentially reducing unnecessary disruptions to normal urban traffic operations. These findings should be interpreted within the context of the considered case study rather than as universally applicable operational conclusions. The results primarily demonstrate the applicability of the proposed two-stage optimization framework under the assumed disaster scenario.

Table 12. Comparative analysis of traffic-control strategies in the first stage.

Traffic-control strategy	Control setting	Latest arrival time (min–max, min)	Computational time (s)	Improvement over no control
No traffic control	All signals operate normally (All 1)	28	5.54	–
Full traffic control	All intersections controlled (All 0)	26	5.55	7.1%
Optimized traffic control (proposed)	Adaptive signal-priority control	26	5.53	7.1%

Table 13. ISO Class 7 Operating Room schedule.

	Stage	y_{1h}^{k}	l_{1h}^{k}	z_{1h}^{k}	w_{1h}^{k}	a_{1h}^{k}
ISO Class 7 Operating Room (OR)	T1	14	5	1	0	14
	T1	16	6	6	0	20
	T1	4	4	6	0	16
	T1	13	5	7	0	20
	T1	6	5	7	0	18
	T1	8	6	7	0	20
	T1	11	7	7	0	20
	T1	7	7	6	0	20
	T1	7	8	6	0	20
	T1	9	8	6	0	20
	T1	8	9	5	0	20
	T1	9	9	5	1	19
	T2	0	7	5	0	15
	T2	0	5	5	2	10
	T2	0	5	3	2	10
	T2	0	5	2	0	10
	T2	0	3	2	1	6
	T2	0	3	1	0	6
	T2	0	2	0	0	4
	T2	0	1	0	0	2
	T2	0	0	0	0	1
	T2	0	0	0	0	0
	T2	0	0	0	0	0
	T2	0	0	0	0	0

Table 14. ISO Class 6 Operating Room schedule.

	Stage	y_{2h}^{k}	l_{2h}^{k}	z_{2h}^{k}	w_{2h}^{k}	a_{2h}^{k}
ISO Class 6 OR	T1	3	1	1	0	3
	T1	15	5	1	6	11
	T1	3	4	1	4	11
	T1	8	4	1	6	11
	T1	10	4	1	9	11
	T1	13	4	1	9	11
	T1	12	4	1	9	11
	T1	4	4	1	7	11
	T1	7	5	1	8	11
	T1	8	5	1	9	11
	T1	10	5	1	10	10
	T1	3	5	1	9	10
	T2	0	5	1	5	10
	T2	0	5	1	1	10
	T2	0	3	1	1	6
	T2	0	2	1	1	4
	T2	0	2	0	0	4
	T2	0	1	0	0	2
	T2	0	0	0	0	1
	T2	0	0	0	0	0
	T2	0	0	0	0	0
	T2	0	0	0	0	0
	T2	0	0	0	0	0
	T2	0	0	0	0	0

Following hospital assignment, injured individuals receive treatment according to the resource availability and operational conditions of the selected hospitals. Patient arrivals at each hospital are assumed to follow a Poisson distribution. The arrival rates of moderately and severely injured patients are determined based on the on-site conditions, with $\lambda_1 = 10, \lambda_2 = 8$. The total time from the accident to the transportation of all injured persons to hospitals is $\Gamma_1 = 120\,\text{min}$, with a first-stage decision interval of $\Delta T_1 = 10\,\text{min}$, resulting in 12 decisions in the first stage. After all injured individuals arrive at hospitals, the total time required to complete treatment is $\Gamma_2 = 360\,\text{min}$, with decisions made every $\Delta T_2 = 30\,\text{min}$, totaling 12 decisions.

The number of injured arriving in each phase of the first stage is calculated using the integral of a Poisson distribution. Combining injury characteristics and historical data, the initial transition probabilities are set as $P_{10} = 0.79, P_{11} = 0.17, P_{12} = 0.04, P_{21} = 0.7, P_{22} = 0.25, P_{23} = 0.05$, with deterioration factors $\delta = 0.03, \theta = 0.07$. After regular scheduling, hospitals allocate beds, doctors, and nurses as medical resources for this traffic accident. Here, the operating room serves as a unit combining doctors, nurses, and beds into one integrated resource. It assumes that an ISO Class 7 Operating Room requires one unit of key resources, while a ten-thousand-level operating room requires three units. The hospital provides a key resource matrix of [25,35]. The unit treatment benefit is $r_1 = 4$ and $r_2 = 6$; the unit ineffective treatment cost is $e_1 = 0.2$ and $e_2 = 0.3$; and the waiting cost per patient is $d_1 = 2$ and $d_2 = 3$.

Unlike pure rule-based scheduling approaches, the proposed second-stage model integrates multiple operational logics simultaneously, including patient arrival order (FCFS), injury severity priority, resource availability, and dynamic deterioration risks. Therefore, FCFS and severe-priority mechanisms are embedded within the optimization process rather than treated as isolated benchmark policies.

The results obtained by MATLAB programming are shown in Table 13 and Table 14.

$$V^{*} = 1178.5$$

When the resource allocation for thousand-level and ten-thousand-level operating rooms is [25,35], the system's total benefit equals 1178.5. When the total resources of thousand-level and ten-thousand-level operating rooms are 25 and 35, respectively, all patients receive treatment. The hospital's system benefit equals 1178.5.

To evaluate the impact of learning and fatigue effects on system performance, we compare the benchmark case with three alternative scenarios. The results are summarized in Table 12 and accompanying figures.

From an operational-cost perspective, which is particularly relevant to public emergency medical systems, the learning effect substantially improves overall system efficiency. Under the "only learning effective" scenario, total operational cost is reduced by 36.26% compared with the benchmark, indicating that experience accumulation enhances service efficiency and resource utilization. In contrast, when only fatigue effects are considered, total cost increases by 26.15%, reflecting substantial efficiency losses caused by human physiological constraints during continuous rescue operations. When both effects are incorporated, total cost still decreases by 17.07% relative to the benchmark, suggesting that the learning effect partially offsets the negative impact of fatigue.

Table 15. Comparison of operational and service performance under different learning and fatigue scenarios.

Scenario	Baseline (no effect)	Only learning effective	Only fatigue effective	Framework effective
Total service effectiveness	1133.4	1365	955.8	1272.4
Relative change (%)	-	20.43%	-15.67%	12.26%
Total operational cost	91	58	114.8	75.467
Relative change (%)	-	-36.26%	26.15%	-17.07%
Average system congestion level	5	4	6	4
Relative change (%)	-	-20.00%	20.00%	-20.00%

In terms of service performance, the average system congestion level decreases by 20% under the learning-only scenario, whereas it increases by 20% when only fatigue is present. When both effects are considered, the average congestion level also decreases by 20% compared with the benchmark. This implies that learning effects mainly contribute to service acceleration and congestion mitigation, while fatigue primarily suppresses service capacity and exacerbates system congestion. Although total benefit follows a similar trend, its interpretation in emergency medical contexts is limited, as it partially overlaps with cost components and does not fully reflect the humanitarian objectives of emergency response systems. Overall, the results demonstrate that ignoring human behavioral characteristics may lead to biased performance evaluation. Although fatigue adversely affects system productivity, sufficiently strong learning effects can partially compensate for these losses and help maintain acceptable operational performance under the current parameter settings.

5.2. Sensitivity analysis

Three-dimensional response surfaces are generated to illustrate the impacts of the learning-effect factor (α_h) and fatigue-effect factor (β_h) on total service effectiveness, operational cost, and average system congestion.

Figure 8 demonstrates the combined effects of learning and fatigue on service effectiveness, operational cost, and average system congestion. Several non-trivial patterns emerge.

From a service effectiveness standpoint, the sensitivity surface displays a distinctly nonlinear architecture. As the learning effect factor α increases, service effectiveness improves markedly, particularly within intermediate ranges. However, this enhancement progressively attenuates at elevated α values, suggesting a learning saturation effect. Beyond this inflection point, additional increments in learning intensity produce diminishing marginal returns. Conversely, the fatigue effect factor (β) exerts a consistently adverse influence on service effectiveness, which intensifies with increasing β. The descending gradient of the surface along the β-axis implies that fatigue functions as a performance inhibitor, counteracting the benefits accrued through learning.

The operational cost surface unveils a more intricate interaction dynamic. At low α values, costs remain comparatively high, owing to prolonged treatment durations and heightened waiting penalties stemming from limited experiential accumulation. As α rises, costs decrease substantially, indicative of enhanced procedural efficiency and optimized resource coordination. Nevertheless, escalating fatigue levels gradually negate these gains, prompting a resurgence in costs. This yields a valley-shaped cost profile, underscoring the presence of an optimal equilibrium zone wherein learning-induced advantages outweigh fatigue-induced detriments. Such a region eludes identification through linear or static modeling approaches, emphasizing the necessity of integrated learning–fatigue management.

A comparable asymmetry is evident in the average system congestion surface. Learning mitigates congestion effectively by expediting patient throughput, whereas fatigue exacerbates it through procedural delays and bottleneck formation. Notably, congestion demonstrates heightened sensitivity to fatigue at higher β values, suggesting that unmanaged fatigue accumulation may precipitate rapid degradation of service stability, even amidst ongoing learning effects.

Figure 9 and Table 15 further clarify these dynamics through single-factor sensitivity analysis. When β is fixed, service effectiveness increases with α in an S-shaped manner, confirming the presence of diminishing returns at higher learning levels. Conversely, when α is fixed, increasing β leads to a nearly monotonic but increasingly steep decline in performance. These results indicate that learning functions as a bounded performance enhancer, while fatigue operates as an accelerating risk factor, emphasizing the need for fatigue-aware scheduling policies.

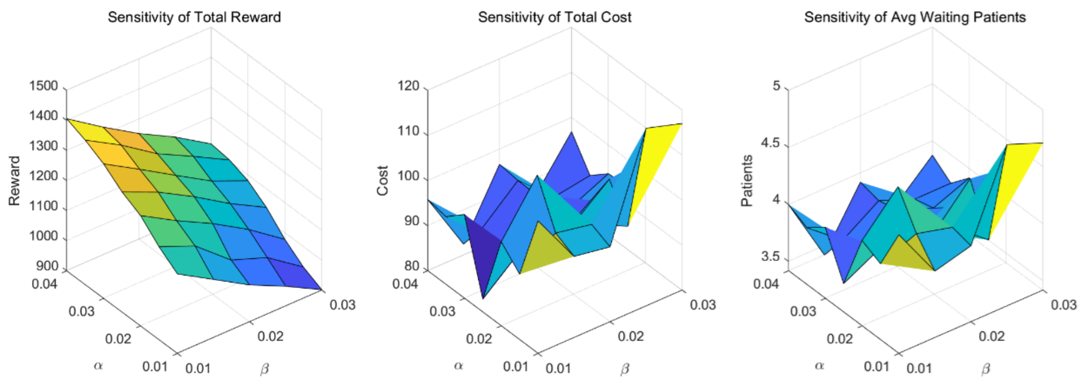

Figure 8. Sensitivity analysis of learning effect factor (α) and fatigue effect factor (β).

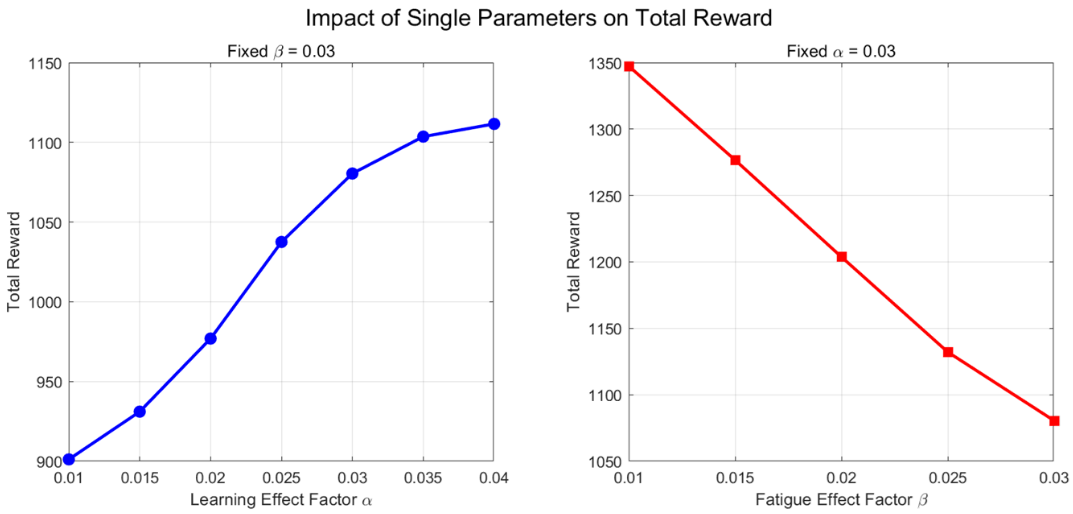

Figure 9. Single-factor sensitivity analysis plot.

Table 16. Single-factor sensitivity analysis.

α_h (β_h = 0.03)	Total reward	β_h (α_h = 0.03)	Total reward
0.01	901.12	0.01	1347.36
0.02	976.92	0.02	1203.71
0.03	1080.45	0.03	1080.45

Figure 10 illustrates the sensitivity of system performance to demand arrival rates. In contrast to the relatively smooth trends observed for learning effects, arrival rates induce structurally distinct growth patterns for both service effectiveness and operational cost.

As arrival rates increase, service effectiveness initially rises rapidly owing to enhanced resource utilization. However, once arrival rates surpass moderate levels, the growth rate decelerates, and the curve gradually plateaus, indicating a concave (logarithmic-like) growth pattern attributable to capacity saturation. Conversely, operational cost escalates at an increasing rate, particularly as arrival rates approach or exceed system capacity. This phenomenon reflects heightened congestion, extended waiting times, and elevated resource consumption.

The divergence between these two curves identifies a critical inflection region: beyond certain arrival-rate thresholds, incremental demand yields diminishing marginal improvements in service performance while incurring disproportionately higher operational costs. This pattern is further substantiated by the average congestion profile, which exhibits sharp increases in waiting times once arrival rates surpass system capacity. Collectively, these findings suggest that demand growth must be managed judiciously and that capacity expansion or operational interventions become necessary when the system approaches saturation.

Notably, an intermediate range of arrival rates corresponds to a sustainable operational regime—characterized by consistently high service effectiveness alongside manageable cost and congestion levels. Identifying this regime is particularly vital for emergency management, as it informs acceptable demand thresholds and serves as an early-warning signal for impending system overload.

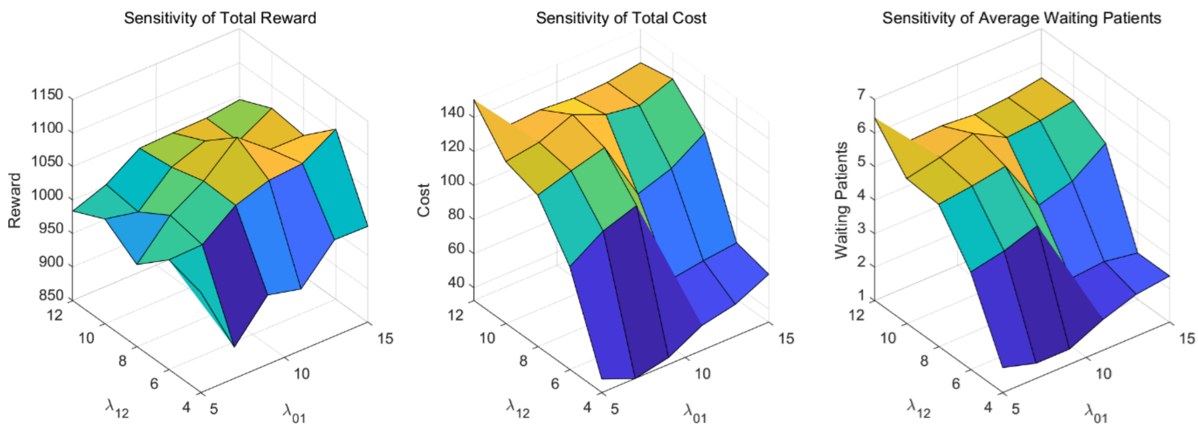

Figure 10. Arrival rate sensitivity analysis plot.

Taken together, the sensitivity analyses reveal that system performance is governed by nonlinear trade-offs and threshold-driven dynamics—not by simple monotonic relationships. Conventional dispatch strategies, which assume fixed service rates or overlook behavioral factors such as learning and fatigue, fail to capture these complexities. In contrast, the proposed optimization framework explicitly incorporates learning and fatigue effects and dynamically adapts resource allocation in real time, thereby enabling precise identification of critical saturation points and delineation of sustainable operating regions.

These insights highlight the necessity of fatigue-aware workforce management, targeted learning enhancement, and demand-responsive capacity planning in emergency medical systems. By pinpointing where marginal benefits decline, and systemic risks escalate, the proposed model delivers actionable, context-sensitive guidance—extending well beyond aggregate performance metrics.

5.3. Sensitivity analysis: managerial implications

Based on the results of the sensitivity analyses, several managerial insights can be derived for emergency medical resource coordination under large-scale disaster scenarios.

First, targeted traffic control may improve emergency response efficiency without requiring blanket signal intervention. The results show that adaptive traffic control achieves the same response completion time as full control while reducing unnecessary disruptions to urban traffic.

Second, learning and fatigue effects exhibit nonlinear characteristics. Learning improves treatment efficiency within a limited range, whereas prolonged fatigue may gradually reduce system performance. This suggests that staff rotation and workload balancing may help maintain operational stability during long-duration emergency response.

Third, dynamic scheduling may enhance system adaptability under growing emergency demand. Compared with static allocation logic, coordinated resource scheduling demonstrates the potential to delay congestion and reduce deterioration risk without immediate physical expansion.

Finally, the results suggest that under large-scale disasters, fully satisfying conventional emergency response standards may be difficult. Therefore, improving emergency-facility coverage and reserve capacity may help strengthen system resilience under high-demand conditions.

6. Conclusions and future work

This paper proposes and demonstrates a two-stage collaborative optimization framework for urban emergency response that integrates emergency resource dispatch and signal-priority traffic control in the first stage with in-hospital treatment scheduling in the second stage. A two-stage optimization model is developed. In the first stage, the coordinated dispatch of fire services and hospitals, together with signal-priority traffic control, is optimized to minimize the response completion time, defined as the latest arrival time among all required rescue resources. In the second stage, a dynamic medical-resource scheduling model incorporating learning and fatigue effects is developed to improve treatment efficiency under evolving emergency conditions. To solve the proposed models, a tailored genetic algorithm (GA) is developed for the first-stage coordinated dispatch and traffic-control problem, while a dynamic programming (DP) approach is employed for the second-stage treatment scheduling problem. The effectiveness of the GA is further verified through comparison with the exact solver Gurobi under the case-study setting. The numerical results demonstrate that learning effects can enhance operational performance, whereas fatigue effects may reduce treatment efficiency during prolonged emergency operations. When both effects are considered simultaneously, the proposed scheduling framework achieves more stable and effective resource utilization than simplified benchmark settings. These findings highlight the importance of incorporating human factors into emergency medical-resource scheduling and support the value of integrated decision-making across different stages of emergency response. Several limitations of this study should be acknowledged. First, the arrival process of injured individuals is represented using simplified assumptions, and more realistic arrival distributions could be incorporated in future research. Second, the deterioration parameters used to characterize injury-state transitions may be further refined using empirical medical data. Third, owing to the substantial uncertainty during the early stages of emergency response, a weak-coupling structure is adopted between emergency dispatch and in-hospital treatment scheduling. Future studies may explore stronger integration mechanisms by incorporating downstream information, such as surgical-resource availability, physician workload, and hospital treatment capacity, into first-stage hospital-selection decisions. Overall, this study provides an integrated optimization framework for coordinating rescue dispatch and medical-resource allocation in urban public emergency events and offers practical decision support for emergency-response planning under resource and traffic constraints.

Author contributions

Shuanglin Li: Conceptualization, methodology, writing—review and editing, supervision, project administration, funding acquisition; Peiyu Kuang: Methodology, software, validation, formal analysis, investigation, data curation, visualization, writing—original draft preparation, writing—review and editing. All authors have read and agreed to the published version of the manuscript.

Use of Generative-AI tools declaration

The authors declare that generative Artificial Intelligence (AI) tools were used during the preparation of this manuscript.

AI tools used: ChatGPT (OpenAI).

How were the AI tools used?

ChatGPT was used solely for English language editing and polishing to improve the clarity, readability, and grammatical quality of the manuscript. No AI tools were used for study design, data collection, data analysis, interpretation of results, or the generation of scientific conclusions.

Where in the article is the information located?

The AI tool was used during the manuscript writing and revision stages, particularly for language refinement throughout the text.

The authors carefully reviewed, revised, and verified all AI-assisted content and take full responsibility for the accuracy, integrity, and originality of the final manuscript.

Acknowledgments

This paper was supported by the National Natural Science Foundation of China, grant number 72474231 and 72074073, and Natural Science Foundation of Hunan Province, grant number 2024JJ5450.

Conflict of interest

The authors declare that there are no conflicts of interest regarding the publication of this paper.

References

1. J. M. Kendra, T. Wachtendorf, Elements of resilience after the World Trade Center disaster: Reconstituting New York City's emergency operations centre, *Disasters*, **27** (2003), 37–53. https://doi.org/10.1111/1467-7717.00218
2. A. H. Chang, S. J. Wang, A. Anandjiwala, E. B. Hsu, A crowd disaster study: The Itaewon Seoul Crush, *Cureus*, **16** (2024), e68811. https://doi.org/10.7759/cureus.68811
3. G. Grasselli, A. Pesenti, M. Cecconi, Critical care utilization for COVID-19 outbreak in Lombardy, Italy, *JAMA*, **323** (2020), 1545–1546. https://doi.org/10.1001/jama.2020.4031

4. Y. Zhang, Z. Li, P. Jiao, S. Zhu, Two-stage stochastic programming approach for limited medical reserves allocation under uncertainties, *Complex Intell. Syst.*, **7** (2021), 3003–3013. https://doi.org/10.1007/s40747-021-00495-7
5. M. T. Gómez-Hernández, M. F. Jiménez, Influence of mentorship on the duration and safety of robotic learning curve for anatomical lung resections, *Video-Assisted Thorac. Surg.*, **6** (2021), 33. https://doi.org/10.21037/vats-21-38
6. K. I. S. Barzani, Ü. Dal. Yılmaz, The relationship between mental workload and fatigue in emergency department nurses, *Cyprus J. Med. Sci.,* **7** (2022), 381–386. https://doi.org/10.4274/cjms.2020.2039
7. V. Bélanger, A. Ruiz, P. Soriano, Recent optimization models and trends in location, relocation, and dispatching of emergency medical vehicles, *Eur. J. Oper. Res.*, **272** (2019), 1–23. https://doi.org/10.1016/j.ejor.2018.02.055
8. N. Andreassen, O. J. Borch, A. K. Sydnes, Information sharing and emergency response coordination, *Saf. Sci.*, **130** (2020), 104895. https://doi.org/10.1016/j.ssci.2020.104895
9. S. Every-Palmer, A. H. M. Kim, L. Cloutman, S. Kuehl, Police, ambulance and psychiatric co-response versus usual care for mental health and suicide emergency callouts: A quasi-experimental study, *Aust. N. Z. J. Psychiatry,* **57** (2023), 572–582. https://doi.org/10.1177/00048674221109131
10. A. O'Brien, G. J. M. Read, P. M. Salmon, Situation Awareness in multi-agency emergency response: Models, methods and applications, *Int. J. Disaster Risk Reduct.*, **48** (2020), 101634. https://doi.org/10.1016/j.ijdrr.2020.101634
11. I. Gago-Carro, U. Aldasoro, D.-J. Lee, M. Merino Maestre, Hierarchical compromise optimization of ambulance locations under stochastic travel times, *Comput. Oper. Res.,* **184** (2025), 107208. https://doi.org/10.1016/j.cor.2025.107208
12. A. Sivagnanam, A. Pettet, H. Lee, A. Mukhopadhyay, A. Dubey, A. Laszka, Multi-Agent reinforcement learning with hierarchical coordination for emergency responder stationing, arXiv:2405.13205, 2024. https://doi.org/10.48550/arXiv.2405.13205
13. I. L. Pitt, The system-wide effects of dispatch, response and operational performance on emergency medical services during Covid-19, *Humanit. Soc. Sci. Commun.,* **9** (2022), 412. https://doi.org/10.1057/s41599-022-01405-z
14. M. Alruwaili, A. Ali, M. Almutairi, A. Alsahyan, M. Mohamed, LSTM and ResNet18 for optimized ambulance routing and traffic signal control in emergency situations, *Sci. Rep.*, **15** (2025), 6011. https://doi.org/10.1038/s41598-025-89651-4
15. D. Duma, R. Aringhieri, Real-time resource allocation in the emergency department: A case study, *Omega*, **117** (2023), 102844. https://doi.org/10.1016/j.omega.2023.102844
16. Y. Y. Xu, S. J. Weng, P. W. Huang, C. H. Chen, Y. T. Tsai, M. C. Tsai, The emergency medical service dispatch recommendation system using simulation based on bed availability, *BMC Health Serv. Res.,* **24** (2024), 1513. https://doi.org/10.1186/s12913-024-12006-8
17. Z. Shen, Y. Tian, Q. Li, D. Li, Y. Zhao, T. Zhou, et al., Enhancing emergency medical service diversion decision-making through large language models integration, *Intell. Med.*, **6** (2026), 56–68. https://doi.org/10.1016/j.imed.2025.04.004
18. Y. Wu, M. Wu, C. Wang, J. Lin, J. Liu, S. Liu, Evaluating the prevalence of burnout among health care professionals related to electronic health record use: Systematic review and meta-analysis, *JMIR Med. Inform.*, **12** (2024), e54811. https://doi.org/10.2196/54811

19. H. Su, Y. D. Zhong, J. Y. J. Chow, B. Dey, L. Jin, EMVLight: A multi-agent reinforcement learning framework for an emergency vehicle decentralized routing and traffic signal control system, *Transp. Res. Part C*, **146** (2023), 103955. https://doi.org/10.1016/j.trc.2022.103955.
20. M. Cao, V. O. K. Li, Q. Shuai, A gain with no pain: Exploring intelligent traffic signal control for emergency vehicles, *IEEE Trans. Intell. Transp. Syst.*, **23** (2022), 17899–17909. https://doi.org/10.1109/tits.2022.3159714
21. Z. Hao, Y. Wang, X. Yang, Every second counts: A comprehensive review of route optimization and priority control for urban emergency vehicles, *Sustainability*, **16** (2024), 2917. https://doi.org/10.3390/su16072917
22. F. Fiedrich, F. Gehbauer, U. Rickers, Optimized resource allocation for emergency response after earthquake disasters, *Saf. Sci.*, **35** (2000), 41–57. https://doi.org/10.1016/S0925-7535(00)00021-7
23. E. Auf der Heide, The importance of evidence-based disaster planning, *Ann. Emerg. Med.*, **47** (2006), 34–49. https://doi.org/10.1016/j.annemergmed.2005.05.009
24. A. M. Caunhye, X. Nie, S. Pokharel, Optimization models in emergency logistics: A literature review, *Soc.-Econ. Plan. Sci.,* **46** (2012), 4–13. https://doi.org/10.1016/j.seps.2011.04.004
25. O. Rodríguez-Espíndola, H. Ahmadi, D. Gastélum-Chavira, O. Ahumada-Valenzuela, S. Chowdhury, P. K. Dey, et al., Humanitarian logistics optimization models: An investigation of decision-maker involvement and directions to promote implementation, *Soc.-Econ. Plan. Sci.*, **89** (2023), 101669. https://doi.org/10.1016/j.seps.2023.101669
26. J. J. Wu, Z. Y. Gao, Emergency support and management of regional integrated traffic system under significant events, *J. Manag. Sci.,* **34** (2021), 67–70. https://doi.org/10.3969/j.issn.1672-0334.2021.06.007
27. J. Qin, Y. Ye, C. Y. Shen, W. Zhang, J. Jian, Optimization method for emergency resource layout for transportation network considering service reliability, *J. Railw. Sci. Eng.,* **15** (2018), 506–514. https://doi.org/10.19713/j.cnki.43-1423/u.2018.02.031
28. H. Liu, Y. Sun, N. Pan, Y. Li, Y. An, D. Pan, Study on the optimization of urban emergency supplies distribution paths for epidemic outbreaks, *Comput. Oper. Res.,* **146** (2022), 105912. https://doi.org/10.1016/j.cor.2022.105912
29. A. M. Caunhye, Y. Zhang, M. Li, X. Nie, A location-routing model for prepositioning and distributing emergency supplies, *Transp. Res. Part E,* **90** (2016), 161–176. https://doi.org/10.1016/j.tre.2015.10.011
30. M. Valaei, A. Saif, H. Sarhadi, H. Afshari, Robust prepositioning and allocation of maritime search and rescue vessels with incident location uncertainty, *Transp. Res. Part E*, **209** (2026), 104693. https://doi.org/10.1016/j.tre.2026.104693
31. Y. Hu, Q. Liu, S. Li, W. Wu, Robust emergency logistics network design for pandemic emergencies under demand uncertainty, *Transp. Res. Part E*, **196** (2025), 103957. https://doi.org/10.1016/j.tre.2024.103957
32. T. Yan, F. Lu, S. Wang, L. Wang, H. Bi, A hybrid metaheuristic algorithm for the multi-objective location-routing problem in the early post-disaster stage, *J. Ind. Manag. Optim*., **19** (2023), 4663–4691. https://doi.org/10.3934/jimo.2022145
33. Y. Gu, Z. Li, H. Liu, Q. Luo, H. Liu, G. Wu, Multi-objective early warning mission planning by multiple satellites using a critical task aggregation-based NSGA-II algorithm, *Adv. Space Res.*, **77** (2026), 11199–11219. https://doi.org/10.1016/j.asr.2025.10.092

34. S. Li, B. Zheng, Simulation research on post-earthquake road network repair schedule under dynamic traffic flows, *Manag. Rev.*, **30** (2018), 3386–3398. https://doi.org/10.16182/j.issn1004731x.joss.201809020
35. S. Li, K. L. Teo, Post-disaster multi-period road network repair: work scheduling and relief logistics optimization, *Ann. Oper. Res.*, **283** (2019), 1345–1385. https://doi.org/10.1007/s10479-018-3037-2
36. S. Li, Z. Ma, K. L. Teo, A new model for road network repair after natural disasters: Integrating logistics support scheduling with repair crew scheduling and routing activities, *Comput. Ind. Eng.*, **145** (2020), 106506. https://doi.org/10.1016/j.cie.2020.106506
37. X. Li, X. Wang, J. Xu, W. Chen, B. Lyu, Integrated emergency vehicle scheduling model in urban emergency rescue within a time-limited period, *Transp. Res. Rec.*, **2678** (2024), 802–818. https://doi.org/10.1177/03611981231209292
38. Z. Li, H. Yu, Z. Zhou, Scheduling of elective operations with coordinated utilization of hospital beds and operating rooms, *J. Comb. Optim.*, **47** (2024), 75. https://doi.org/10.1007/s10878-024-01167-1
39. L. Yu, Z. Yang, A two-stage robust optimization model for the location-allocation-rostering problem of emergency service facilities under demand uncertainty, *SSRN Electronic Journal.*, 2025. https://doi.org/10.2139/ssrn.5704777
40. U. Ozdemir, S. Mete, M. Gul, A two-stage volunteer assignment model for post-disaster search and rescue operations, *Sci. Rep.*, **16** (2026), 11159. https://doi.org/10.1038/s41598-026-41627-8
41. H. Liu, Y. P. Tsang, C. K. M. Lee, C. H. Wu, K. L. Yung, Optimizing UAV flocks for emergency response in post-disaster industrial zones, *IEEE Trans. Ind. Inform.*, **22** (2026), 37–48. https://doi.org/10.1109/tii.2025.3608299
42. M. Cao, J. Peng, L. Yang, Y. Yang, Multi-UAV task allocation and path planning in emergency rescue scenarios with uncertain requirements, *J. Ind. Manag. Optim.*, **21** (2025), 6107–6133. https://doi.org/10.3934/jimo.2025124
43. Y. Xiong, Y. Zhou, J. She, A. Yu, Collaborative coverage path planning for UAV swarm for multi-region post-disaster assessment, *Veh. Commun.*, **53** (2025), 100915. https://doi.org/10.1016/j.vehcom.2025.100915
44. W. Luo, J. Yao, R. Mitchell, X. Zhang, W. Li, Locating emergency medical services to reduce urban-rural inequalities, *Soc.-Econ. Plan. Sci.*, **84** (2022), 101416. https://doi.org/10.1016/j.seps.2022.101416
45. Z. Wan, Q. Liu, C. Ye, W. Liu, Research on hospital emergency resource dynamic allocation model under emergencies, *Comput. Appl. Res.*, **37** (2020), 456–459, 469. https://doi.org/10.19734/j.issn.1001-3695.2018.07.0529
46. Y. Ni, L. Zhao, Study on deployment of emergency medical resources with injury condition consideration, *Logist. Technol.*, **34** (2015), 115–118, 129. https://doi.org/10.3969/j.issn.1005-152X.2015.05.036
47. X. Pan, Q. Liu, C. Ye, Study on decision making of medical emergency resource allocation considering the degree of injured wounded, *Syst. Sci. Math.*, **39** (2019), 1159–1170. https://doi.org/10.12341/jssms13670
48. M. Rabbani, N. Oladzad-Abbasabady, N. Akbarian-Saravi, Ambulance routing in disaster response considering variable patient condition: NSGA-II and MOPSO algorithms, *J. Ind. Manag. Optim.*, **18** (2022), 1035–1062. https://doi.org/10.3934/jimo.2021007

49. M. Du, A data-driven decision-making approach for joint mass screening and pharmaceutical resource allocation in epidemic outbreak, *China Manag. Sci*., **32** (2024), 168–179. https://doi.org/10.16381/j.cnki.issn1003-207x.2021.2214
50. H. Zhang, W. Zhou, Y. Sun, Joint allocation of emergency medical resources with time-lag correlation during cross-regional epidemic outbreaks, *Comput. Ind. Eng.,* **164** (2022), 107895. https://doi.org/10.1016/j.cie.2021.107895
51. P. S. Chen, Y. J. Lin, N. C. Peng, A two-stage method to determine the allocation and scheduling of medical staff in uncertain environments, *Comput. Ind. Eng*., **99** (2016), 174–188. https://doi.org/10.1016/j.cie.2016.07.018
52. A. Stefanini, D. Aloini, E. Benevento, R. Dulmin, V. Mininno., A data-driven methodology for supporting resource planning of health services, *Soc.-Econ. Plan. Sci.*, **70** (2020), 100744. https://doi.org/10.1016/j.seps.2019.100744
53. L. Yu, H. Yang, L. Miao, C. Zhang, Rollout algorithms for resource allocation in humanitarian logistics, *IISE Trans.*, **51** (2019), 887–909. https://doi.org/10.1080/24725854.2017.1417655
54. T. Y. Ho, S. Liu, Z. B. Zabinsky, A multi-fidelity rollout algorithm for dynamic resource allocation in population disease management, *Health Care Manag. Sci.*, **22** (2019), 727–755. https://doi.org/10.1007/s10729-018-9454-6
55. W. Yu, M. Jia, X. Fang, Modeling and analysis of medical resource allocation based on Timed Colored Petri net. *Future Gener. Comput. Syst.,* **111** (2020), 368–374. https://doi.org/10.1016/j.future.2020.05.010
56. A. Boostani, F. Jolai, A. Bozorgi-Amiri, Designing a sustainable humanitarian relief logistics model in pre- and postdisaster management, *Int. J. Sustain. Transp.,* **15** (2021), 604–620. https://doi.org/10.1080/15568318.2020.1773975
57. T. Cai, Y. Ye, Delivering fresh produce during a lockdown: The post-pandemic pickup and distribution problem with time constraints, *Soc.-Econ. Plan. Sci*., **103** (2026), 102383. https://doi.org/10.1016/j.seps.2025.102383
58. A. Batista, J. Vera, D. Pozo, Multi-objective admission planning problem: a two-stage stochastic approach, *Health Care Manag. Sci.*, **23** (2020), 51–65. https://doi.org/10.1007/s10729-018-9464-4
59. J. Tang, Y. Wang, An adjustable robust optimisation method for elective and emergency surgery capacity allocation with demand uncertainty, *Int. J. Prod. Res.*, **53** (2015), 7317–7328. https://doi.org/10.1080/00207543.2015.1056318
60. B. Addis, G. Carello, E. Tanfani, Evaluating the impact of the level of robustness in operating room scheduling problems, *Healthcare*, **12** (2024), 2023. https://doi.org/10.3390/healthcare12202023
61. N. Chikhi, B. Djehiche, Patients transportation in surgery scheduling problem, *J. Syst. Sci. Complex*., **37** (2024), 1100–1113. https://doi.org/10.1007/s11424-024-3073-8
62. J. J. Wang, Z. L. Dai, X. W. Hou, Operating room scheduling for elective patients under cross-department resource sharing, *Syst. Eng. Theory Pract*., **41** (2021), 2947–2962. https://doi.org/10.12011/SETP2020-1804
63. G. Bektur, H. K. Aslan, Artificial bee colony algorithm for operating room scheduling problem with dedicated/flexible resources and cooperative operations, *Int. J. Optim. Control Theor. Appl.,* **14** (2024), 193–207. https://doi.org/10.11121/ijocta.1466
64. H. X. Tong, Q. Z. Liu, X. M. Pan, Operating rooms scheduling optimization under emergency, *Math. Pract. Theory*, **49** (2019), 141–147.

65. Y. Y. Feng, I. C. Wu, T. L. Chen, Stochastic resource allocation in emergency departments with a multi-objective simulation optimization algorithm, *Health Care Manag. Sci*., **20** (2017), 55–75. https://doi.org/10.1007/s10729-015-9335-1
66. B. Akbarzadeh, B. Maenhout, A two-layer heuristic for patient sequencing in the operating room theatre considering multiple resource phases, *Comput. Oper. Res.*, **170** (2024), 106768. https://doi.org/10.1016/j.cor.2024.106768
67. ISO, ISO 14644-1:2015 Cleanrooms and associated controlled environments Part 1: Classification of air cleanliness by particle concentration, 2015. Available from: https://www.iso.org/standard/53394.html.
68. World Health Organization, Global guidelines for the prevention of surgical site infection, 2016. Available from: https://iris.who.int/bitstream/handle/10665/250680/9789241549882-eng.pdf.
69. H. Bavafa, J. O. Jónasson, The distributional impact of fatigue on performance, *Manag. Sci.,* **70** (2023), 3319–3337. https://doi.org/10.1287/mnsc.2023.4855
70. Ministry of Emergency Management of PRC, 14th Five-Year Plan for emergency rescue force construction, 2022. Available from: https://www.mem.gov.cn/gk/zfxxgkpt/fdzdgknr/202206/t20220630_417326.shtml.
71. National Health Commission of the People's Republic of China, Guiding opinions on further improving pre-hospital medical emergency services, 2020. Available from: https://www.nhc.gov.cn/wjw/c100175/202009/07e1ddf9a8ee40b5a45dc8c89b5cd3c3.shtml.